Miner Deposita (2007) 42:879–899
DOI 10.1007/s00126-007-0138-2

ARTICLE

Geological context, mineralization, and timing of the Juramento sediment-hosted stratiform copper–silver deposit, Salta district, northwestern Argentina

C. Gustavo Durieux · Alex C. Brown

Received: 3 August 2006 / Accepted: 4 April 2007 / Published online: 8 May 2007

Abstract The Juramento deposit in northwestern Argentina exhibits several readily visible general characteristics of sediment-hosted stratiform copper (SSC) mineralization. It consists of fine-grained disseminated base-metal sulfides within marine to lacustrine graybeds (the basal whitish Late Cretaceous Lecho Sandstone and shallow-water carbonates of the overlying Maastrichtian Yacoraite Formation) that overlie a thick sequence of redbeds (the Pirgua Subgroup). The property has been examined and drilled in three successive exploration programs as a possible analog of world-class mineralization in the copperbelts of central Africa and the Kupferschiefer. The present report provides specific field and laboratory results that confirm the classification as SSC-type mineralization. The host graybeds are the basal sandstone and overlying oolitic and stromatolitic units of the Yacoraite Formation, which are shown from textural studies to be carbonaceous and to have initially contained very fine-grained, disseminated, syndiagenetic pyrite. These sediments would have been sufficiently porous and permeable in early diagenetic time to allow an infiltration of metalliferous fluids from the underlying redbeds, resulting in the observed progressive replacement of in situ pyrite by common base-metal sulfides (sphalerite, galena, argentiferous tetrahedrite, and copper-rich sulfides: first chalcopyrite, then bornite, and finally chalcocite). Sulfur isotope analyses indicate that a portion of the sulfur of ore-stage sulfides is isotopically heavier than that of pyrite, possibly due to a contribution from associated gypsum. Ore-stage sulfides are zoned vertically and obliquely through the mineralized zones, from cupriferous sulfides at low stratigraphic levels to lead- and zinc-rich mineralization above, with unreplaced pyrite remaining within upper Yacoraite strata. The zoned sulfides and their replacement textures, the peneconformable configuration of the mineralized zones, and the position of ore-stage mineralization adjacent to a stratigraphically defined redox transition from redbeds upward into graybeds indicate an overprint of copper (and accompanying ore-stage metals) on originally pyritic graybeds. The influx of ore-stage metals, presumably in an oxidized low-temperature brine, terminated with a silicification event that effectively sealed the host carbonates. These observations and the overall genetic interpretation are consistent with the general deposit-scale genetic model for early diagenetic SSC mineralization. The regional geologic context is also consistent with its classification as a SSC deposit: It is hosted by post-oxyatmoversion sediments and was formed in association with evaporites at a low paleolatitude in a major intracontinental rift system.

Keywords Sediment-hosted stratiform copper · Sulfur isotopes · Juramento · Salta · Argentina

Editorial handling: B. Lehmann

C. G. Durieux (✉) · A. C. Brown
Department of Civil, Geological and Mining Engineering,
École Polytechnique de Montréal,
P.O. Box 6079, Station Centre-Ville,
Montreal, Quebec H3C 3A7, Canada
e-mail: gdurieux@angloamerican.ca

A. C. Brown
e-mail: acbrown@polymtl.ca

Present address:
C. G. Durieux
Anglo American Exploration (Canada) Ltd.,
Suite 800 - 700 West Pender St.,
Vancouver, British Columbia V6C 1G8, Canada

Introduction

The research presented in this paper was undertaken (a) to provide a basic description of the relatively unknown Juramento copper–silver deposit situated in Upper Cretaceous intracontinental rift-basin sediments in the Salta district, northwestern Argentina (Fig. 1), (b) to explain the genesis of this mineralization, and (c) and to determine whether this deposit qualifies as sediment-hosted stratiform copper (SSC) mineralization such as that found in the Central African Copperbelt or in the Kupferschiefer of Europe. The first formal proposal that the mineralization was of the SSC type led to mapping and diamond drilling in 1980 by Pecomrio, a subsidiary of RioCanex. Most of the drilling was limited to near-surface zones of oxide and mixed oxide–sulfide mineralization characterized by malachite–azurite staining. However, many fundamental characteristics of SSC mineralization (e.g., fine-grained disseminated cupriferous sulfides in carbonate units overlying redbeds) were confirmed, and an enticing sub-economic deposit was outlined (~9 million tonnes, grading about 1% copper and 20 g/t silver). Subsequently, Espisúa and Amengual (1983) and Sureda et al. (1986) also assigned the Juramento mineralization to the SSC deposit type.

Mason (1996) recommended renewed exploration both on the Juramento property and in surrounding areas exhibiting similar lithologic sections, emphasizing the potential for economic primary sulfide mineralization of the SSC type beneath the supergene oxidation zone. A report by Kirkham (1996) also supported the continued use of the SSC model as an exploration guide during the field mapping and drilling by Paramount Ventures and Finances (1996–1998). Paramount outlined 11 million tonnes of drill-indicated mineralization in two zones (El Plomo and El Cobre), extending over stratigraphic thicknesses of several meters and having an overall grade of 0.83% copper and 19.2 g/t silver (Rotzien and Wormald 1998). Alexander Mining (2005) has recently carried out further drilling, with the intent to define an open-pit mining operation based on recalculated reserves of 44.7 Mt grading 0.8% Cu and 21.8 g/t Ag.

Thus far, the Juramento copper–silver deposit is the most economically promising of numerous occurrences of SSC mineralization in the Upper Cretaceous Salta Group sedimentary rocks in the Salta and Jujuy provinces of northwestern Argentina. By 1996, these widespread occurrences of sediment-hosted copper were correlated with an extensive intracontinental rift system (Fig. 1), as have most other SSC deposits (Jowett 1989; Kirkham 1989; Brown

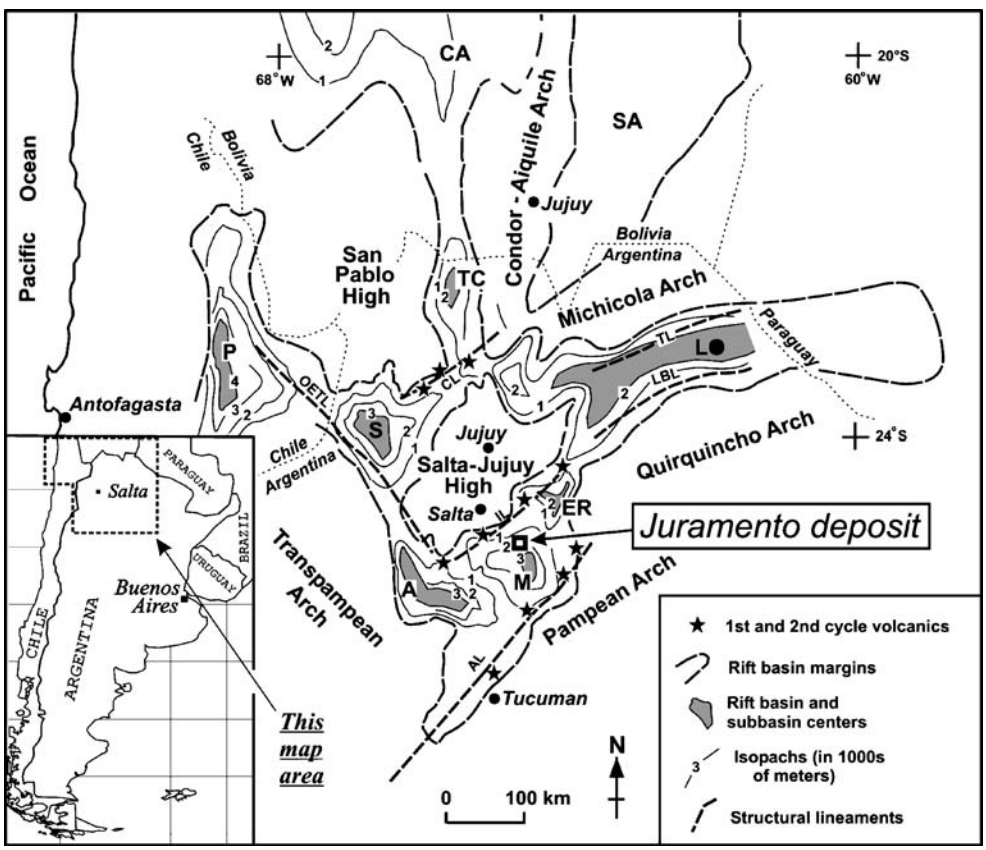

Fig. 1 Location of the sediment-hosted Juramento copper–silver deposit within the Metán Late Mesozoic Salta intracontinental rift system of northwestern Argentina. The rift system surrounds the Salta–Jujuy High and extends into adjacent Chile, Bolivia, and Paraguay. Rift basins: *A* Alemania, *CA* Central Andean, *ER* El Ray, *LO* Lomas de Olmedo, *M* Metán, *P* Purilactis, *S* Sey, *SA* SubAndean, and *TC* Tres Cruces. Regional lineaments define some basin margins: *Al* Aconquija, *CL* Cobres, *IL* Isonza, *OETL* Olacapato–El Toro. Volcanic centers are recognized along some lineaments. Modified after Salfity (1979) and Salfity and Marquillas (1994)

1992). The widespread sediment-hosted mineralization was labeled the "Salta copperbelt" (Kirkham 1996), coincident with its extensive intracontinental rift system and hopefully emulating the famous copperbelt of the Democratic Republic of the Congo and Zambia, and the renowned Kupferschiefer copperbelt of Poland and Germany.

To test the validity of this exploration model, Mason engaged the current authors in field and laboratory studies to be carried out in parallel with Paramount's exploration program. The first author was employed in the field for a total of 10 months; the remainder of his masters-level research was conducted at l'École Polytechnique de Montréal under the supervision of the second author. The present report describes (1) the tectonic and sedimentary contexts of the mineralization; (2) the mineralogy, textures, paragenesis, and zoning of the primary sulfides; and (3) the timing of mineralization relative to the deposition of the host sediments, to their subsequent diagenesis, and to their deformation during Andean orogenesis.

Prior publications pertinent to our work include the studies of several other researchers (see, for example, those cited above), especially those describing broad topics such as the progressive development of geological environments in central South America since Precambrian time, the development of extensive Late Mesozoic–Early Tertiary rift basins across this area, and the local conditions of syn- and post-rift sedimentation in those basins. Much of this information is found in geological reports prepared by government and university services and in publications of scientific societies. An important portion of our understanding of the regional geology of the area also derives from petroleum exploration and development that have focused on the same Cretaceous rift-basin sediments as those hosting the Juramento copper–silver deposit.

Regional geologic setting

At the subcontinental scale, the Juramento deposit is located within the Sub-Andean Range, which comprises the easternmost portion of the N/S-trending Andean Cordillera (Fig. 2). Progressively farther westward are (1) the Eastern Cordillera, composed mainly of Precambrian basement and Paleozoic sediments tectonically thrust eastward over post-Mesozoic sediments; (2) the Altiplano (Puna), consisting of sheets of Precambrian and Paleozoic sediments thrust over Tertiary continental rocks; and (3) the Main Cordillera (Western Cordillera), exceeding 6,000 m in altitude at the Argentina–Chile border and consisting primarily of Late Tertiary and Quaternary volcanoes and volcanic flows. To the east of Juramento, Mesozoic, Tertiary and Quaternary sediments occur in the Sub-Andean

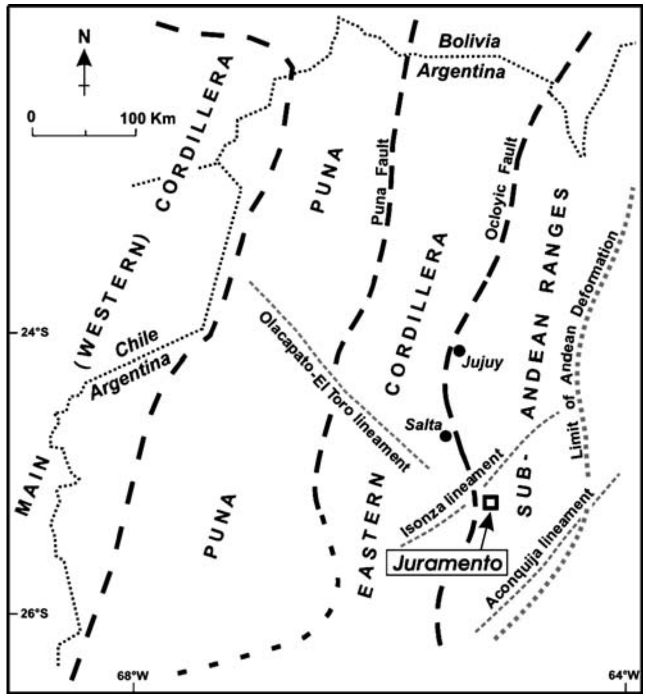

Fig. 2 Physiographic domains of northwestern Argentina. The Juramento deposit lies at an altitude of about 1,350 to 1,550 m within the Sub-Andean Ranges (principally from Mon and Salfity 1995)

Range (including the Chaco–Paraná Basin) and further eastward across the Precambrian South American craton.

The roots of the Andes Mountain chain were formed during the late Proterozoic Brasiliano cycle of the Pan-American orogeny (800–600 Ma). Major structural lineaments that developed at this time are considered to have played repeated roles in controlling continental-scale compressional and extensional displacements throughout the following Hercynian (Late Paleozoic) and Andean (Mesozoic–Cenozoic) orogenic cycles (see, for example, Mon and Salfity 1995). The Andean cycle has been and continues to be closely related to the subduction of the Pacific oceanic crust beneath the South American continental plate.

A widespread intracontinental rift system developed east of the Main Cordillera in Late Jurassic–Early Cretaceous time (Araucan orogeny), coincident with the global-scale breakup of Gondwana and the opening of the proto-Atlantic ocean. A major portion of this rift system, the Salta Basin, occurs in northwestern Argentina; other branches extend into Chile (where the Yacoraite Formation equivalent is the Quebrada Blanca Formation), Bolivia (where the Yacoraite Formation equivalent is the El Molino Formation), Peru, and Paraguay (Fig. 1). The Salta Basin rifts were filled largely by Lower to Upper Cretaceous syn-rift redbeds interlayered with minor bimodal basalts, and then by uppermost Cretaceous post-rift sandstones and carbonates (Fig. 3). The final fill of the rift depocenters consists of

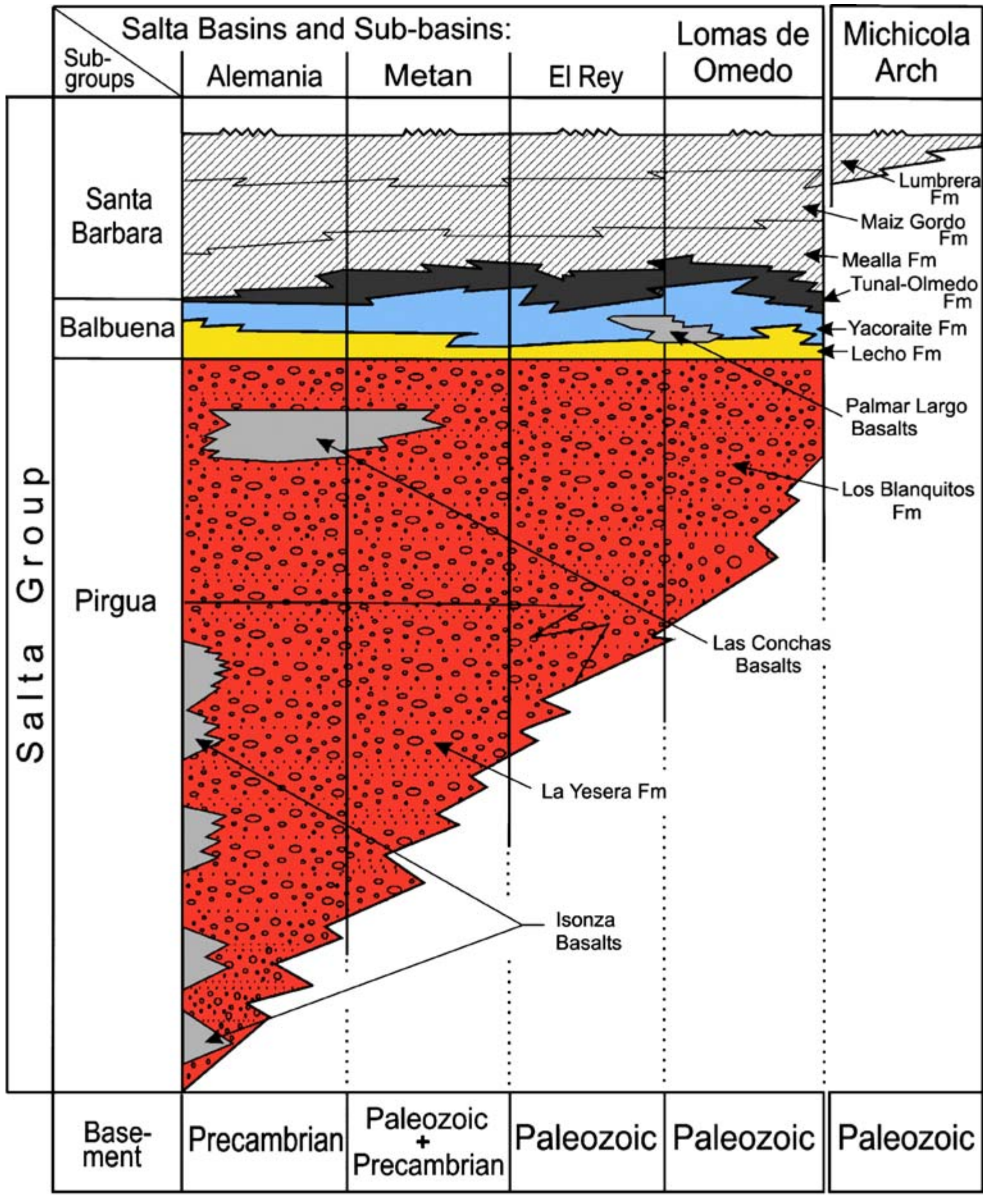

Fig. 3 Stratigraphy and inter-basin correlation of the Salta Group sedimentary and volcanic strata among the principal depocenters of the Salta rift-basin system and across the Michicola Arch (principally after Marquillas and Salfity 1988; Salfity and Marquillas 1994)

Paleocene–Eocene fluvial–lacustrine sediments. Rift inversion occurred during the Late Eocene–Early Oligocene Inca compressional event. Later, the Quechua (Early to Late Miocene) and Diaguita (Pliocene–Pleistocene) disturbances folded and faulted the Cretaceous and Tertiary sediments of the Salta Basin, reactivating pre-Cretaceous lineaments in the basement (Jordan and Alonso 1987; Salfity and Marquillas 1994; Mon and Salfity 1995).

The Salta Basin is composed of several rift segments or sub-basins surrounding the Salta–Jujuy High (Fig. 1). The sub-basin margins are defined by regional-scale lineaments and by northeast-trending arrays of volcanic centers coincident with those lineaments. The Juramento property is located to the southeast of the Salta–Jujuy High, in the Cretaceous Salta Group of the Metán depocenter.

Stratigraphy of the Metán sub-basin

Salta Group sedimentation began in the Metán sub-basin with the deposition of syn-rift continental redbeds interlayered with mafic volcanics in Early to Mid-Cretaceous time (Pirgua Subgroup; Fig. 3; Marquillas 1984; Palma 1984; Marquillas and Salfity 1988; Marquillas et al. 1984). The conformably overlying post-rift sedimentary section (Balbuena Subgroup) is composed of Late Cretaceous shallow-water shore-clastic and carbonate sediments composed of a basal sandstone (Lecho Formation) that grades rapidly upward into shallow marine or lacustrine carbonates and siltstones (Maastrichtian Yacoraite Formation). Rift-fill sedimentation culminated in the early Tertiary with the deposition of greenish fluvial–lacustrine siltstones and evaporites (Tunal–Olmedo Formation), and reddish continental claystones and siltstones (Mealla, Maiz Gordo, and Lumbrerea formations).

The northwestern and southeastern margins of the Metán depocenter are delineated by the Isonza and Aconquija lineaments, respectively, along which mafic volcanic strata were deposited during the accumulation of more than 3,000 m of syn-rift Pirgua redbeds (Figs. 1 and 3). In the Juramento area, near the northwestern margin of the Metán sub-basin, the thickness of the post-rift Lecho and Yacoraite sediments is about 240 m and increases toward 400 m in the central portions of the sub-basin. The Juramento mineralization is located mainly in the basal shallow-water carbonates and fine-grained clastics of the Yacoraite Formation and, to a lesser extent, in the immediately subjacent portions of the Lecho sandstone.

General property-scale geography and geology

The Juramento deposit is located in northwestern Argentina (65°7′W, 25°13′S), about 60 km southeast of the city of Salta, and is readily accessible via national highways and local dirt roads. The topography is hilly, varying in elevation from about 800 to 2,800 m, with slopes attaining 35° in some places. The climate is semi-arid, and vegetation is sparse. The principal exposures of stratiform mineralization are found on three ridges (Cerros del Cobre and del Plomo, and the Condor Ridge; Fig. 4), all of which may be reached by all-terrain vehicles. Petroleum is produced from a well located 15 to 20 km from the Juramento property; the Yacoraite Formation, which hosts the majority of the Juramento copper–silver deposit, is also considered both a source rock and a reservoir rock for the hydrocarbons of the Metán sub-basin, with significant petroleum production at depth northeast of Juramento (Mon and Salfity 1995).

The geology of the Juramento property is dominated by slices of Cretaceous sedimentary rocks thrust up and folded onto a Late Precambrian–Devonian basement, which was deformed intensely during the Late Paleozoic Hercynian orogeny. The valley between Cerro del Cobre and Cerro del Plomo is occupied by Pirgua redbeds, whereas the ridges are generally represented by the more

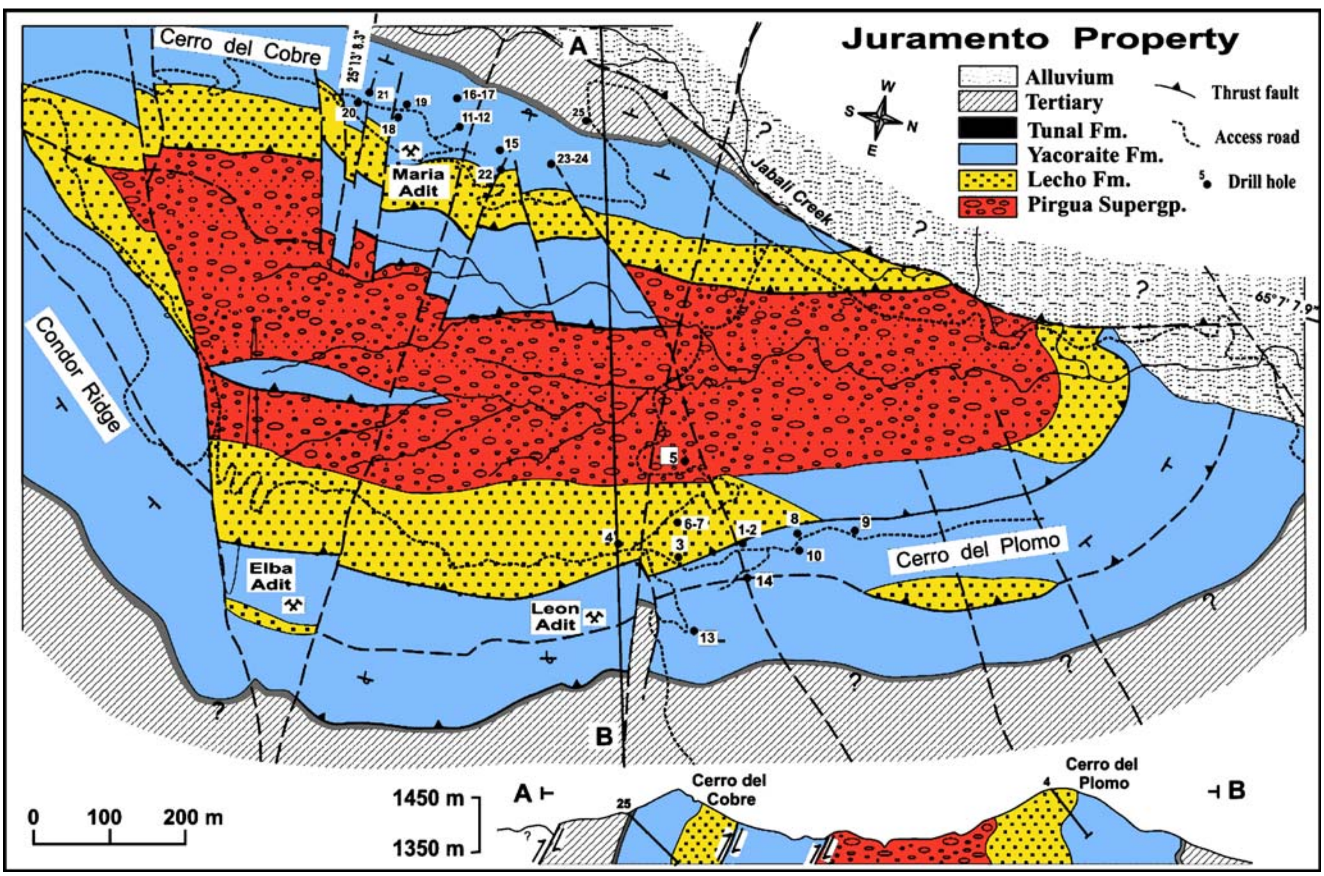

Fig. 4 Geological map and cross-section of the Juramento property, as determined from detailed surface mapping and exploration drilling (modified after Rotzien and Wormald 1998). Sediment-hosted copper–silver mineralization occurs in the basal Yacoraite Formation and the subjacent Lecho Formation, principally on the Cerro del Cobre and the Cerro del Plomo–Condor ridges. ARC asks if we should give credit to the geos who did the mapping

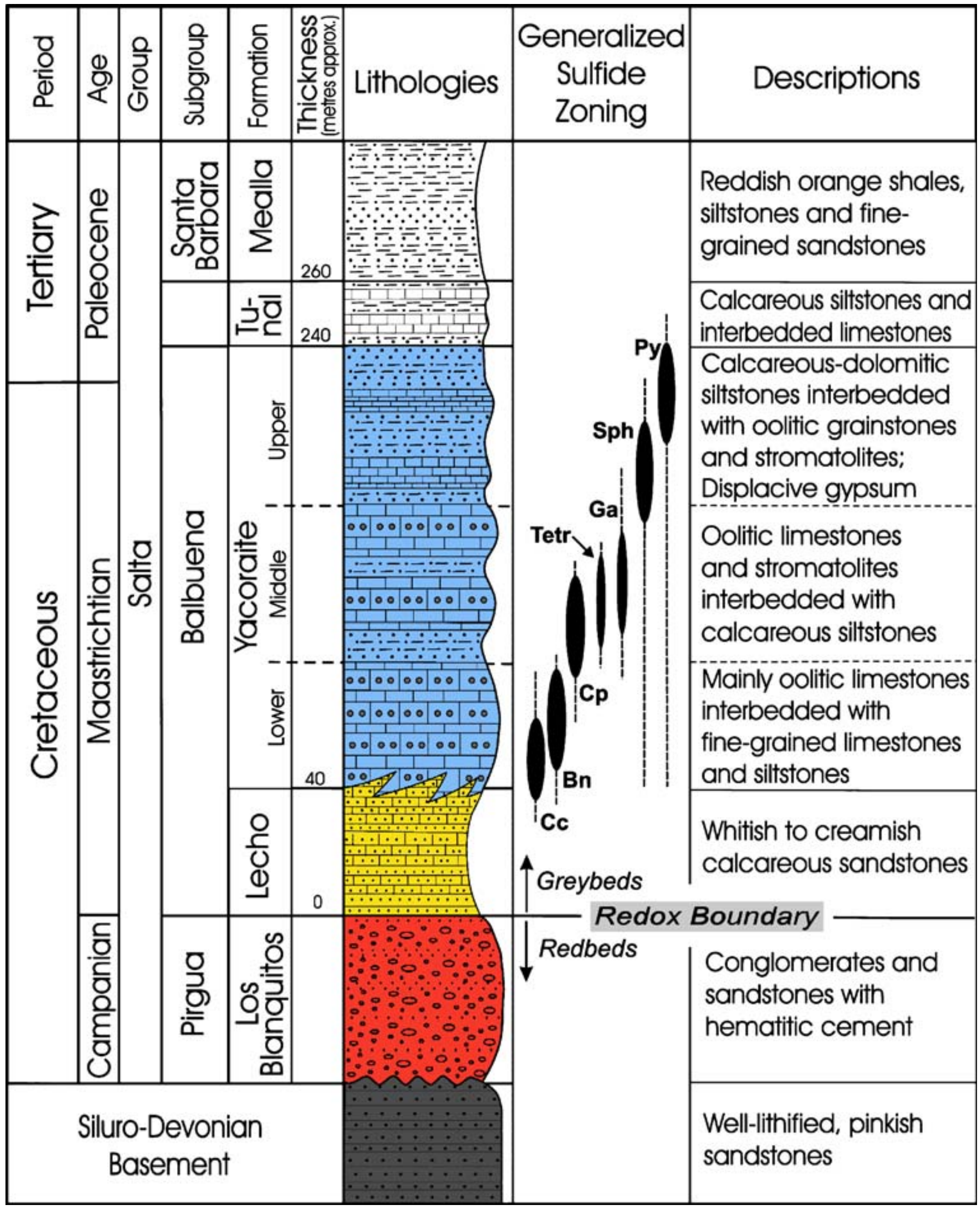

Fig. 5 Stratigraphic column for the Juramento property, also showing the general zoning of sulfides, from copper-rich compositions in basal units to lead and zinc sulfides at intermediate levels, and syndiagenetic pyrite in overlying portions of the Yacoraite Formation

resistant Yacoraite carbonate rocks. The lithologic compositions of the stratigraphic units and subunits on the property, as well as their average thicknesses, are indicated schematically in Fig. 5.

The occurrence of copper mineralization on the property is evident from abundant malachite–azurite staining on weathered rock surfaces. Highly mineralized outcrops may also have visible disseminated galena and/or cupriferous sulfides as well as their oxides. Drilling by Paramount to depths attaining 150 m typically encountered well-preserved primary sulfide mineralization beyond depths of 50 to 70 m. From deep sections of drill core, it has been possible to recognize the primary sulfide mineralogy, textures, and zoning (Durieux 2000), and to calculate the thicknesses and grades of zones of primary stratiform mineralization (Rotzien and Wormald 1998).

Host-rock petrology and petrography

An understanding of the genesis of SSC mineralization generally requires a close examination of both the host graybeds and the underlying footwall redbeds (see, for example, descriptions and interpretations in Boyle et al. 1989; Brown 1997a, 2003, 2005; Kirkham 1995; Hitzman et al. 2005). At Juramento, the footwall redbeds are composed of the coarse-grained reddish clastic sediments of the Pirgua Subgroup, and the graybeds are represented by the overlying whitish Lecho sandstone and the grayish Yacoraite carbonates and siltstones (see Fig. 5).

Pirgua subgroup

The Pirgua redbeds are composed of distinctly reddish, coarse- to fine-grained clastic sedimentary rocks having a silty matrix and a calcitic–hematitic cement. The principal mineral constituents of the subrounded to subangular clasts are quartz, K-feldspar, plagioclase, pyroxene, muscovite, and tourmaline. The thick accumulation of redbeds in local depocenters measuring >1,000 m in depth (Fig. 1) and the immaturity of the clasts, both in morphology and composition, indicate a local source typical of intracontinental rift redbeds. Petrographic studies by Zielinski et al. (1983), Walker (1989), and Ryan et al. (1989) show that the pervasive hematitic cement of such redbeds results from the early diagenetic alteration of mafic mineral constituents of immature redbed clasts, presumably during infiltration of oxygen-rich meteoric water.

Lecho formation

About 40 m of friable, whitish, calcareous Lecho sandstone, composed largely of quartz, feldspar, muscovite, and tourmaline in a calcitic microspar matrix, forms the upward conformable transition from Pirgua redbeds to the overlying Yacoraite carbonates and siltstones. Remnant micrite in the matrix preserves rolled algal material and pellets that contain very fine-grained disseminated (in part framboidal) pyrite. Terrigenous grains are rounded to subrounded and may be coated by radial carbonate overgrowths. Where the terrigenous debris is less abundant, allochems (ooids, oncoids, and lumps) are common, as are a micritic carbonate cement and a microspar matrix. The environment of Lecho deposition was probably that of a broad, sinking, shallow-water plain.

The Lecho sandstone may be mineralized with a largely interstitial sulfide cement (mainly chalcocite and/or bornite), especially in its uppermost portions immediately underlying the Yacoraite Formation (Fig. 5). Where well mineralized, supergene alteration has produced a greenish (malachite) stain on the otherwise whitish Lecho sandstone.

Yacoraite formation

The Yacoraite carbonate–siltstone unit is the principal host of copper–silver mineralization at Juramento. It is approximately 200 m thick and lies in high topographical relief because of the relative resistance of carbonate rocks in semi-arid climates. On fresh surfaces, it is grayish in color, but may be buff to orange-yellow on weathered exposures as a result of oxidized pyrite, or greenish (malachite-stained) due to the oxidation of cupriferous sulfides. Fractures containing black hydrocarbon tars are common.

Shallow-water facies of the Yacoraite Formation include grainstone, packstone, wackestone, mudstone, stromatolitic boundstone, siltstone, marl, and intraformational conglomerate. Oolites are generally abundant in the lower Yacoraite and less common in upper sections, whereas finely layered stromatolitic beds are common in upper sections.

Grainstones are generally composed of calcite-coated oolitic and oncolitic grains that have been partially to completely dolomitized (Fig. 6a). Ooids are generally large (commonly 400 to 1,800 μm in diameter) and sparitic, with radial or concentric cortices of one layer or more; rims may be bored. In some cases, the cores are formed of microfossils or terrigenous clasts; other allochems include intraclasts, macro- and microfossils, pelloids, and lumps. Some macroscopic samples appear to be oolitic, but under the microscope, they are found to have concentric algal growth layers characteristic of oncolites. Intergranular and rim cements are composed of sparite, microsparite, and/or dolosparite. A thin meniscus-type calcitic cement overgrowing ooids suggests

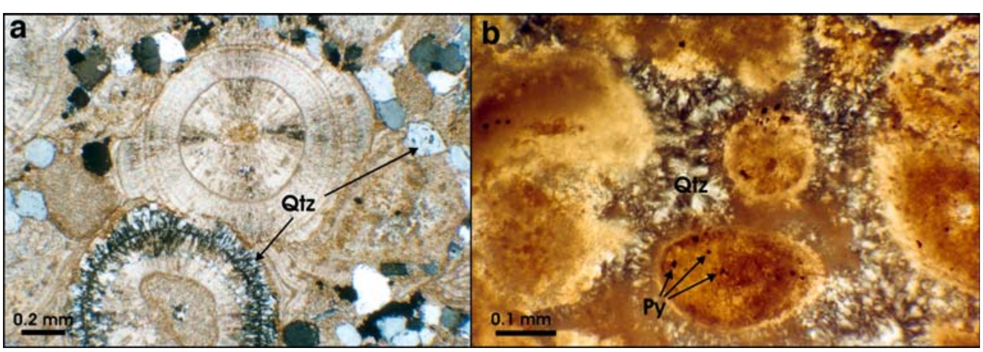

Fig. 6 **a** Oolitic grainstone showing radial cortice partially replaced by quartz (*Qtz*), suggesting replacement before transformation of the ooid rim to a more stable calcite. Note that ooids otherwise resisted burial compaction, but experienced pressure solution at the contacts between ooids. Authigenic quartz also occurs as discrete grains around ooids. Cross-polarized, transmitted light. **b** Megaquartz filling the interparticular porosity. Very fine-grained pyrite (*Py*) is included in ooids. Plane-polarized, transmitted light

frequent subaerial exposure. Micrite is generally absent as a matrix, but micritized ostracods, pelecypods, and gasteropods are common. The permeability of grainstones was probably high due to fabric-selective intraparticule and mouldic porosities.

Packstones of the Yacoraite Formation resemble grainstones in hand specimens, but in thin sections, they are found to have micritic matrices and to contain small oolitic and pelletic allochems (Fig. 6b) surrounded by larger oolitic allochems measuring up to 2 mm in diameter. The terrigenous fraction is minor. Micritic pellets and small ooids (up to 200 μm in size) are generally well sorted. Packstones also contain a variety of recognizable fossils such as ostracods, gasteropods, pelecypods, foraminifera, algae, and phosphatic debris probably derived from fish. Intraclasts (<3% of the rock volume) are typically irregular in shape and may surpass 2 mm in size. Some limestone clasts have intergranular sparitic, microsparitic, and/or dolomicritic cements; the cements may be vadose, having formed during subaerial exposure. The packstone porosity is mouldic and less than that of the Yacoraite grainstones.

Wackestones are characterized by abundant micritic and dolomicritic matrices, accompanied by patches of sparite. The porosity, represented only by vesicular, interparticular, and fracture spaces, was poor.

In most cases, the Yacoraite mudstones are formed of thinly laminated calcitic micrite and dolomicrite, although bioturbation is generally pervasive. Fossils and allochems composed of calcitic gasteropods, pelloids, ostracods, and algal fragments are common. The porosity is of a fenestral or vesicular type. Where bioturbated, the mudstone porosity should have been high before advanced compaction.

Stromatolitic boundstones consist of calcareous and dolomitic algal laminations alternating with layers of silt or sand (Fig. 7). Both fine-grained and coarse-grained pyrites are commonly included. Clastic layers may contain fossils (e.g., ostracods), oolites, pellets, and other allochems. The porosity in stromatolitic boundstones was fenestral.

Siltstones and marls form the finest-grained facies of the Yacoraite Formation. Siltstones, composed mainly of thinly laminated silt with an argillic matrix and calcareous cement, are abundant toward the top of the Yacoraite Formation. The principal mineral components are quartz and feldspar in the coarse silt fraction and phyllosilicates in the argillaceous matrix. Marls, on the other hand, are more abundant in the lower Yacoraite. They have a dark-gray color compared to the siltstones and are composed of clays with calcareous cement. Siltstone porosities would have been effectively non-existent after minor compaction.

Intraformational conglomerates form a minor constituent of the Yacoraite Formation, but are distributed across its entire thickness. They are commonly formed of angular or subangular clasts, 1 to 5 mm in size; the matrix is typically composed of silt-size detrital quartz and feldspar grains. The cement is dolomitic and/or calcitic.

Although commonly referred to as a simple carbonate unit, the Yacoraite Formation varies from high-energy facies (grainstones and packstones) to low-energy facies (wackestones, siltstones, and mudstones), with an overall gradation from predominantly calcareous sediments in the basal portions of the Yacoraite Formation and more siliciclastic sediments in upper sections. Examined more closely, the grainstones and packstones are characterized by oolitic and oncolitic grains and by graded beds typical of wave-dominated high-energy environments (Greensmith 1989). The fine parallel-laminated nature of the mudstones suggests deposition in calm and/or restricted environments. The mudstones are commonly burrowed, a feature also typical of calm or restricted environments of sedimentation such as those found either in shallow lagoons or at levels beneath wave action in deeper water (Greensmith 1989). Because the allochems of associated wackestones are oncoids or concentric algal concretions, the preferred

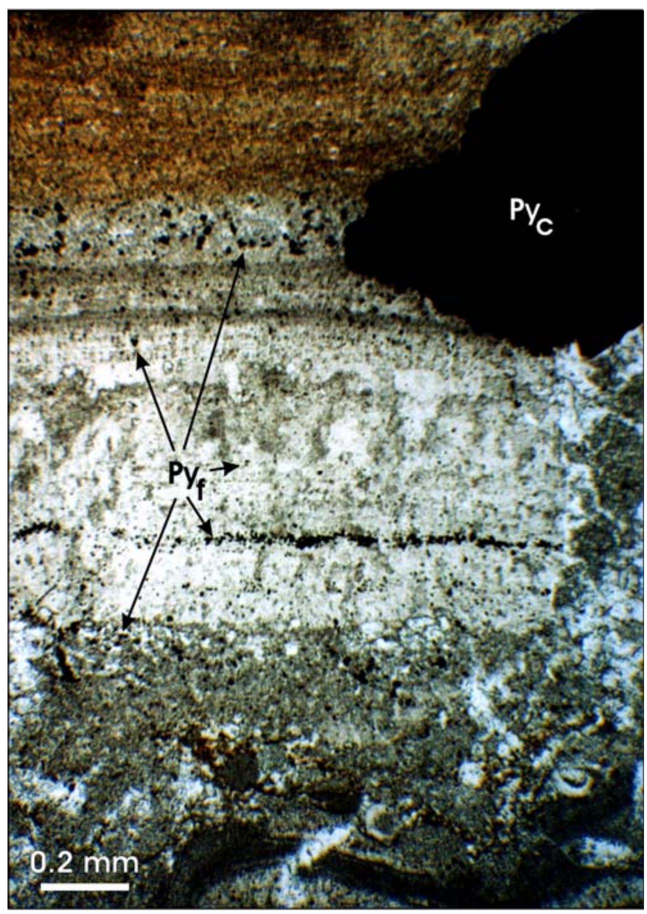

Fig. 7 Dolomitic stromatolitic boundstone, with very fine-grained pyrite (*Py$_f$*) along microlaminations, and coarse-grained aggregate of pyrite (*Py$_c$*) against which microlaminae were deformed during burial compaction. Plane-polarized, transmitted light

environment of sedimentation would be that of a lagoon protected by sandbars.

Transitions upward from high-energy carbonate facies to low-energy pelagic clastic facies are typically abrupt, whereas the transitions from low-energy to high-energy facies are gradual (Fig. 8). The many transitions from low- to high-energy sediments form repeated shallowing-upward sequences characteristic of stable carbonate platforms where the rate of sedimentation would have exceeded the rate of subsidence and where successive sediments would have been deposited in progressively shallower waters (Friedman and Sanders 1978; Friedman et al. 1973, 1992; James 1984; Tucker and Wright 1990). Such shallowing-upward sequences are found especially in lacustrine low-gradient ramp margins (Tucker and Wright 1990), as in the lacustrine Eocene Green River Formation of the western USA (Williamson and Pickard 1974) and in the modern lake sediments of the East African Rift (Kendall 1969; Reading 1982; Platt and Wright 1991).

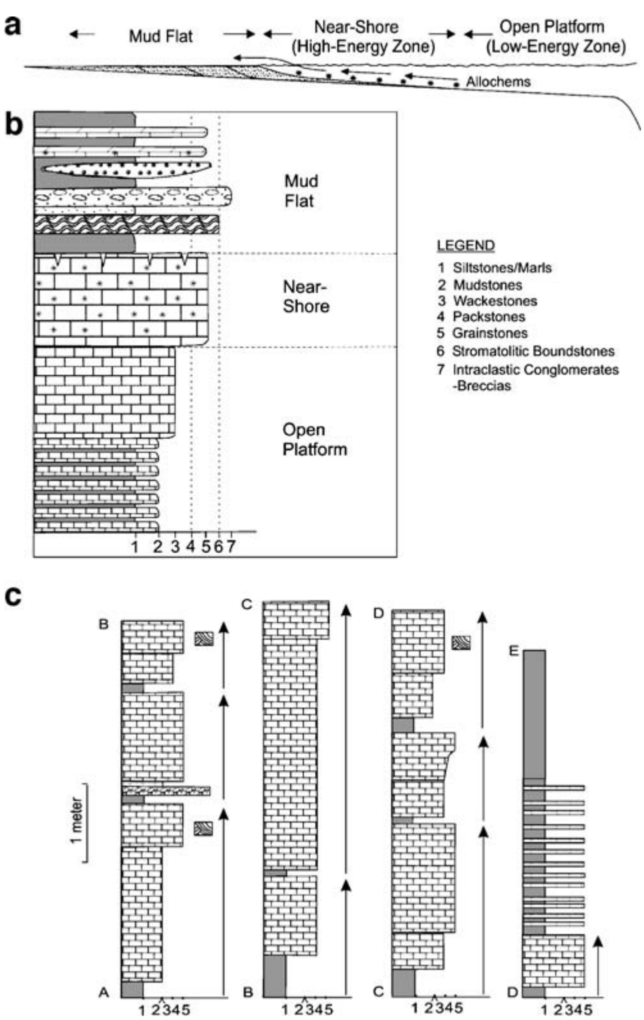

Fig. 8 Shallowing-upward sequences. **a** Sedimentary environments, after James (1984). **b** Generalized shallowing-upward sequences and interpreted environments recognized in the Yacoraite Formation. **c** Shallowing-upward sequences (*arrows*) identified in the vicinity of the Leon adit

Pre-ore, ore-stage, and post-ore petrographies

Petrographic studies were undertaken on the various facies of the Yacoraite Formation and their fabrics in an attempt to bracket the timing of emplacement of ore-stage sulfides relative to four successive events in the history of the Juramento host rocks: sedimentation, diagenesis, tectonic deformation, and supergene oxidation. Figure 9 summarizes the relative timing of particular features and events, including ore-stage mineralization and other mineral emplacements, as recognized in this petrographic study.

Pyrite, a pre-ore sulfide

Unmineralized, unoxidized portions of the Yacoraite Formation are characterized by disseminations of fine- to coarse-grained pyrite. Although coarse-grained pyrite is readily visible, it is not the dominant textural type; abundant very fine-grained pyrite provides a more pervasive amount of iron sulfide, most of which cannot be observed except in polished sections. Thus, two textural types are recognized: (1) very fine-grained (typically up to 15 μm in size) disseminations of pyrite, in part framboidal (Fig. 10a and b) and (2) coarse-grained euhedral pyrite and aggregates of pyrite grains (commonly 25 μm to 1 mm or more in size; Fig. 7).

At the microscopic scale, very fine-grained pyrite is seen to be principally associated with carbonaceous matter, ooids, and laminations of apparent algal origin. In detail, it is dispersed between the multiple cortex layers of ooids, between the layers of encrustation in oncoids, along algal laminations of stromatolites (occupying their fenestral porosity), and throughout carbonaceous mudstones. Fine disseminations of pyrite may outline recrystallized shells or allochems, and in some cases, they have been recognized in thin moulds of micrite, including sediments that were micritized before the deposition of sparry cements. In some highly carbonaceous siltstones, very fine-grained pyrite occurs in concentrations of up to 30 or 40% in thin bands along bedding planes. High concentrations of very fine-grained pyrite are also found in bioturbations where pelloids were an important source of organic matter that, in turn, supported anoxic bacterial activity and bacterial reduction of sulfates. Besides framboidal aggregates, very fine-grained pyrite may also form nodular aggregates (up to 1 cm in size) in interparticulate spaces. Very fine-grained pyrite is considered to be syndiagenetic in origin (Fig. 9), having formed in the earliest unconsolidated sediment from sulfide produced by

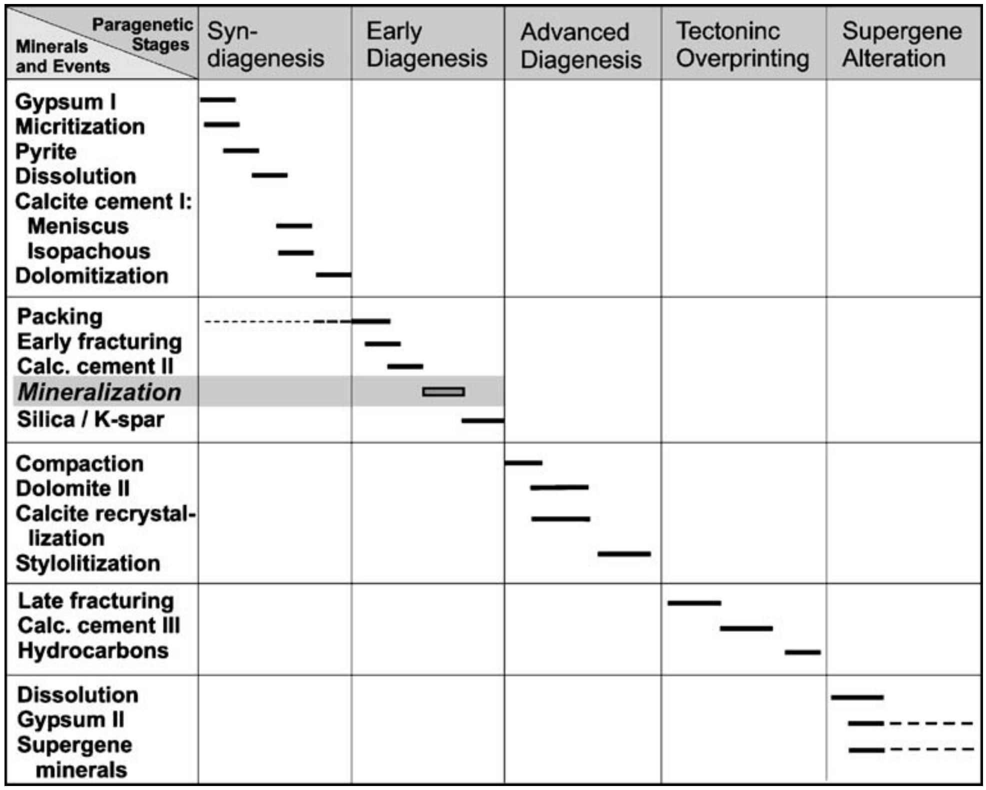

Fig. 9 Sequence of minerals formed and associated events identified in the petrography of the Yacoraite Formation hosting copper–silver mineralization. The *horizontal axis* is divided from left to right into progressive stages: syndiagenesis, for very early diagenetic effects, that take place in a sediment soon after deposition and at very shallow burial; early diagenesis, for effects at moderate burial; advanced diagenesis, for effects at deep burial, followed by tectonic effects (e.g., deformation, fracturing) resulting principally from Andean orogenesis; and recent supergene alteration of the host rock and mineralization

bacterial sulfate reduction; the sulfide reacted, in turn, with iron normally available in impure sediments to form iron sulfides that matured into syndiagenetic pyrite.

Coarse-grained euhedral pyrite typically occupies intergranular spaces. Aggregates of very fine-grained pyrite may be partially or wholly annealed to form coarse-grained euhedral pyrite, suggesting that coarse-grained pyrite was formed during advanced diagenetic recrystallization of very fine-grained pyrite that may have accompanied sediment compaction and/or tectonic pressures.

Ore-stage zinc, lead, copper-iron, and copper sulfides

The dominant primary ore-stage mineralization at Juramento consists of disseminated sulfides, mainly in the coarser-grained host facies (grainstone and packstone) of the Yacoraite Formation. A minor amount occurs in compact siltstone and mudstone; local concentrations also occur in the porous burrowed portions of mudstone. Primary cupriferous sulfides also occur as a cement (principally chalcocitic) in the uppermost whitish-gray Lecho sandstone. Ore sulfides may be visible to the naked eye, but are best seen with the aid

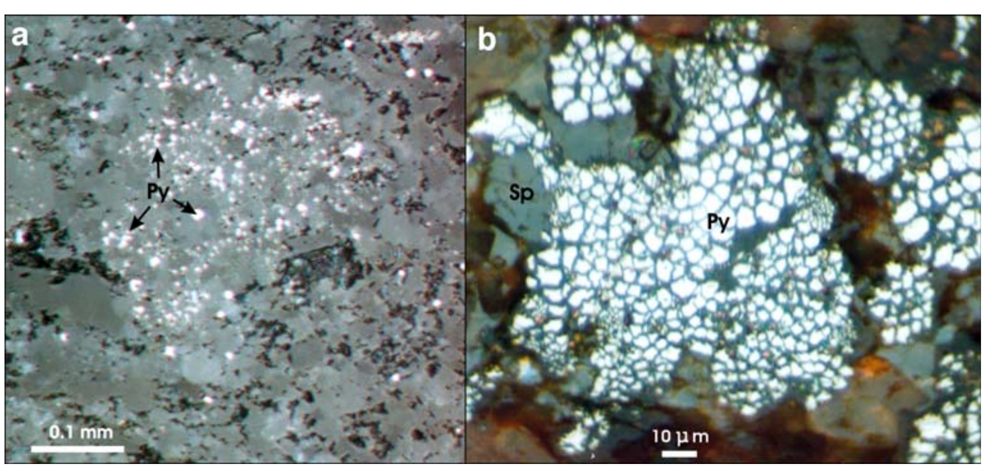

Fig. 10 Fine-grained pyrite: **a** Disseminated, **b** Framboidal groupings. Reflected, plane-polarized light; **b** under oil immersion

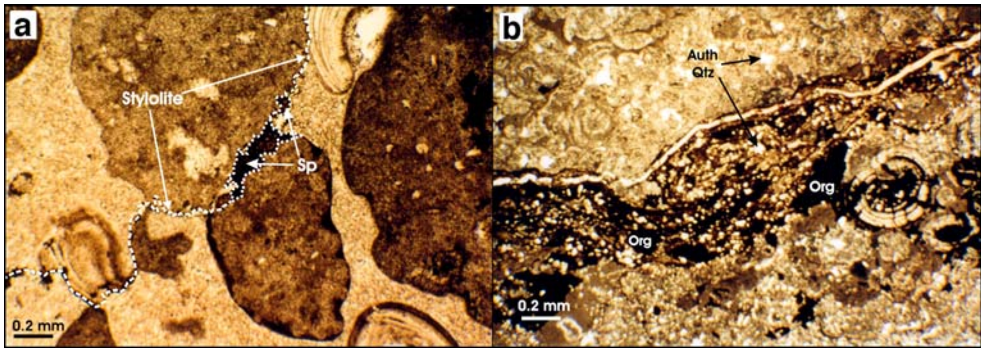

Fig. 11 **a** Remnant sphalerite along a stylolite. **b** Organic matter concentrated along a stylolite. Transmitted, plane-polarized light

of a hand lens. Details are most readily seen in polished sections.

As described below, the cupriferous sulfides (chalcocite, bornite, chalcopyrite, and tetrahedrite) and the associated zinc and lead sulfides (sphalerite and galena) formed at a distinctly later stage of diagenesis than the syndiagenetic pyrite described above. These ore-stage sulfides are discussed in the order of their appearance in a generalized paragenetic sequence: sphalerite→galena→(tetrahedrite)→ chalcopyrite→ bornite→chalcocite.

Sphalerite is present across much of the Yacoraite Formation, especially in the upper and middle sections of the formation if cupriferous sulfides occur in the basal section. Its abundance typically decreases in the uppermost Yacoraite Formation where pyrite predominates. It is found largely as irregular disseminated grains ranging up to 100 μm in size in siltstones to more than 2 mm in size in the intragranular and mouldic porosity of grainstones. In transmitted light, large grains may exhibit growth layers and may include small opaque material interpreted to be sulfides or organic matter. They also have fluid inclusions generally measuring less than 5 μm in size. Sphalerite also occurs in microveinlets (5 to 15 μm wide and up to 2 mm in length) and as fillings of primary (e.g., intragranular pores and burrows in mud) and in secondary (e.g., mouldic) pore spaces. Grains of sphalerite are found along stylolites, probably formed as a residue during the development of this secondary porosity (Fig. 11a); insoluble organic matter, other sulfides, and authigenic quartz also accumulated along stylolites (Fig. 11b).

Disseminated sphalerite is typically associated intimately with fine-grained disseminated pyrite and galena, to a lesser extent with tetrahedrite and chalcopyrite, and rarely with bornite and chalcocite. It encloses and replaces pyrite (Fig. 12a), in some cases, forming pseudomorphs after pyrite euhedra, and it is replaced in turn by galena (Fig. 12b) and less commonly by cupriferous sulfides (Fig. 12c). Evidence of sphalerite replacement is found mainly in the form of embayed remnants of sphalerite enclosed by rims of galena.

Exceptionally, the sphalerite core is surrounded first by a zone of chalcopyrite, then by an outer zone of galena. This zoning sequence suggests that chalcopyrite deposition preceded the deposition of galena, contradicting the more common and expected paragenetic sequence (sphalerite→ galena→chalcopyrite) described above. However, upon closer examination (e.g., using a 40× or stronger oil immersion objective lens), the outer zone of galena is

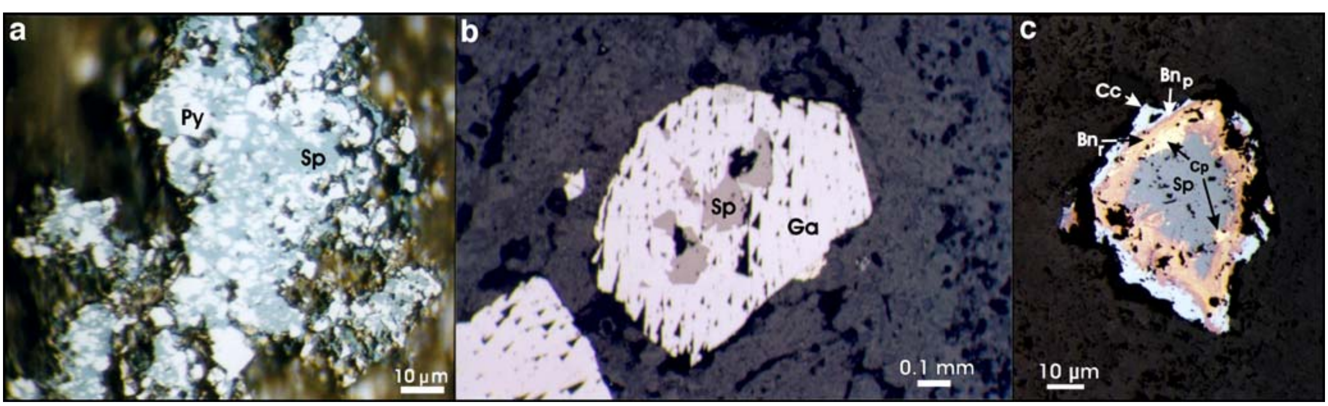

Fig. 12 **a** Fine-grained pyrite, partially replaced and enclosed by sphalerite (*Sp*). **b** Sphalerite partially replaced by galena (*Ga*). **c** Sphalerite progressively replaced by chalcopyrite (*Cp*), Bornite (Bn_p, purplish; Bn_r, pink varieties), and chalcocite (*Cc*). Reflected, plane-polarized light; **a** and **c**, under oil immersion

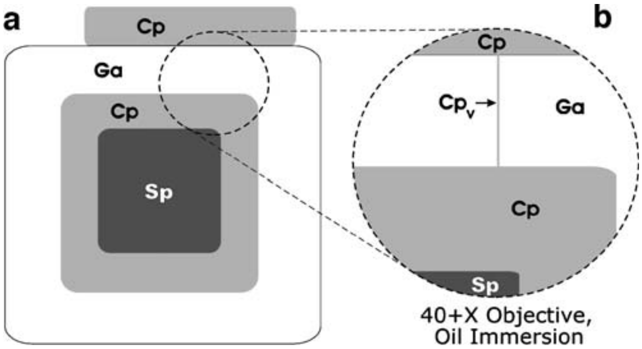

Fig. 13 **a** Schematic illustration of the *apparent* progressive replacement of sphalerite (*Sp*), first by chalcopyrite (*Cp*), then by galena (*Ga*), as seen with a low-power objective. **b** Higher resolution view with a high-power objective and oil immersion reveals that a chalcopyrite microveinlet (Cp_v) connects the intermediate chalcopyrite zone to the external chalcopyrite grain. See text for the explanation and implications of this texture

found to be cut by minute veinlets of chalcopyrite connecting the inner chalcopyrite zone to more chalcopyrite surrounding the zoned sulfide grain, indicating that chalcopyrite is consistently post-galena (Fig. 13). The unusual position of a chalcopyrite zone between the sphalerite core and its outer zone of galena may be explained by the relative instabilities of the zinc, lead, and copper sulfides: If a grain of sphalerite had been partially replaced by galena and then the pore solution became cupriferous, the invading copper should have replaced sphalerite in preference to galena because sphalerite is the least stable sulfide of the pair sphalerite–galena. The access of copper to the sphalerite core could have occurred by the observed microveining across the galena zone (Fig. 13b) or possibly by solid-state diffusion of copper across the galena zone. One additional conclusion may be drawn from this texture: The mineralizing pore fluid was devoid of copper, while the lead-bearing fluid deposited galena; otherwise, sphalerite would have been replaced directly by chalcopyrite rather than by galena.

Galena overlaps the base of the overlying sphalerite-dominant zone and continues into the lower strata of the Yacoraite Formation. It is generally found in abundance in the upper middle Yacoraite and in rare amounts in the upper Yacoraite. Pyrite may still be found in close association with galena, but in general, the abundance of pyrite is minor compared to the relative abundance of pyrite above the lead- and zinc-rich zones. Where cupriferous sulfides are minor or absent in the basal Yacoraite, galena is the dominant sulfide in the lower Yacoraite. Thus, its occurrence is broadly zoned between that of sphalerite above and cupriferous sulfides below.

Galena is commonly observed as disseminated grains ranging from about 40 μm to 1 or 2 mm in size and as replacement rims on sphalerite (Fig. 12b), especially in primary intragranular pores and burrows and in secondary mouldic pores. It is also found as inclusions in chalcopyrite, bornite, and tetrahedrite, particularly in the lower portions of the Yacoraite Formation where cupriferous sulfides may be common. Galena may exhibit deformed cleavages, possibly suggesting an emplacement before compaction of the host sediment or, more probably, before or during Andean tectonic deformation. Espisúa and Amengual (1983) report negligible amounts of silver in galena.

Tetrahedrite is the only significantly silver-bearing mineral at Juramento. The composition, determined by X-ray diffraction and microprobe analyses by Espisúa and Amengual (1983), is richer in antimony than arsenic, and thus, it is referred to as tetrahedrite in this paper. Although not obvious in hand specimens or drill core samples because of its minor occurrence and its intergrowths with other sulfides, it is readily found in polished sections containing chalcopyrite and galena (Fig. 14). It occurs mainly as small grains associated with chalcopyrite and galena replacing sphalerite, and is considered contemporaneous with the transition from galena to chalcopyrite deposition.

Chalcopyrite generally overlaps occurrences of galena and sphalerite described above and becomes the dominant sulfide at levels stratigraphically lower than occurrences of lead and zinc sulfides. Remnants of pyrite may still occur in the upper levels of chalcopyrite mineralization.

Chalcopyrite occurs as isolated disseminated anhedral grains and aggregates, and as pseudomorphs after both very fine-grained pyrite and laths of gypsum (Fig. 15). Individual grains range up to 200 μm in size. Pseudomorphs after gypsum laths, ranging up to 1 to 2 mm in length, are found in the primary intergranular porosity of the grainstone where the gypsum cement had sealed the pores, together with a late dolomicritic cement. These pseudomorphs are only weakly deformed (flattened ooids and spalled cortices)

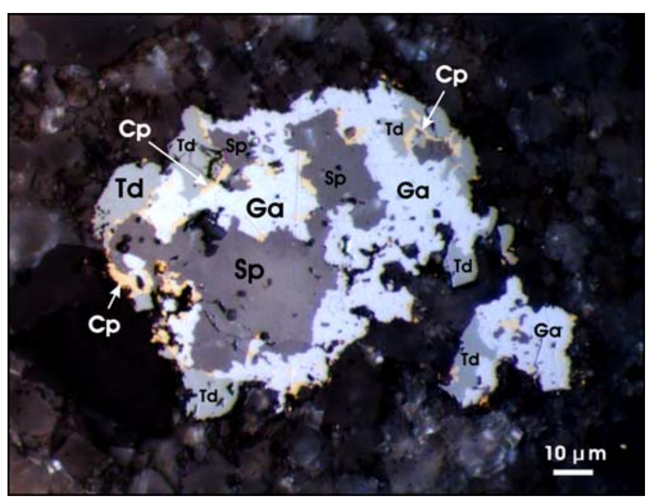

Fig. 14 Sphalerite (*Sp*) replaced by an assemblage of galena (*Ga*), tetrahedrite (*Td*), and chalcopyrite (*Cp*). Reflected, plane-polarized light; oil immersion

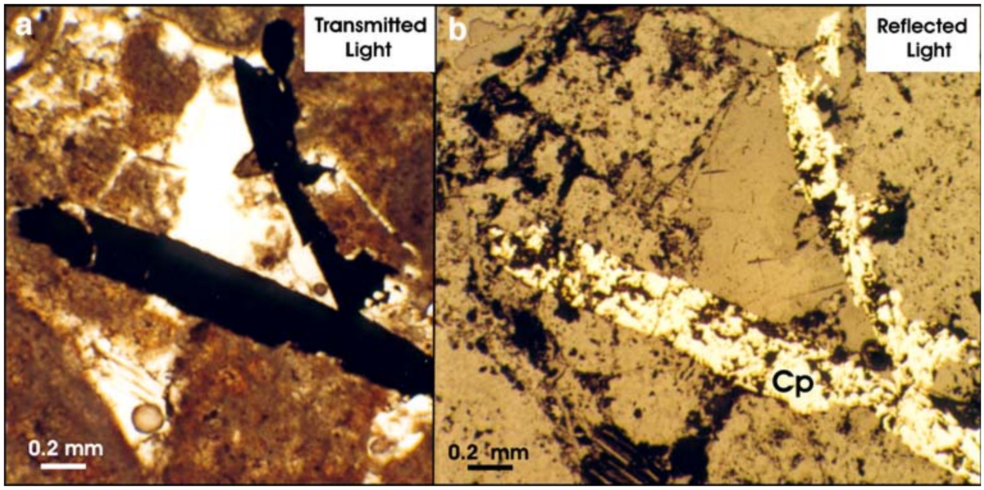

Fig. 15 Blades of gypsum replaced by chalcopyrite (*Cp*). **a** Transmitted, plane-polarized light. **b** Same gypsum pseudomorphs, viewed in reflected, pane-polarized light

compared to the strongly compacted allochems seen in the same samples. Chalcopyrite was also observed in stylolites following bedding planes; in a few cases, the stylolites abruptly crosscut stratigraphy and were mistaken for veinlets in earlier reports, giving rise to the false impression that the emplacement of copper mineralization at Juramento could have been structurally controlled.

Chalcopyrite replaces earlier sulfides (especially sphalerite and galena; see above) and commonly includes remnants of those minerals as well as tetrahedrite. The close association of tetrahedrite and chalcopyrite, the occurrence of tetrahedrite inclusions in chalcopyrite (see above), and the absence of chalcopyrite inclusions in tetrahedrite suggest that the two sulfides were deposited closely together in time, with tetrahedrite emplacement generally preceding that of chalcopyrite. Chalcopyrite is replaced in turn by the more copper-rich sulfides, bornite and chalcocite. A basket-weave intergrowth of very fine-grained chalcopyrite may occur in some bornite (see below).

Bornite is typically found in the lower and lowermost middle Yacoraite Formation. It is generally observed as irregular disseminated grains and as pseudomorphs after very fine-grained euhedral pyrite. Irregular grains of bornite commonly occupy primary intergranular and secondary diagenetic porosities. As with other sulfides, bornite may be concentrated along stylolites. Aggregates of irregular grains of bornite vary in size up to 800 μm in diameter.

Two distinct varieties of bornite are noted: a “purple” bornite that is typically sulfur-poor and copper-rich, and a “pink” (or anomalous) bornite that is typically sulfur-rich (Brett and Yund 1964; Yund and Kullerud 1966; Ramdohr 1969). The two bornites are vertically zoned, with the pink variety more abundant in the upper portions of the overall bornite zone. Pink bornite may exhibit a basket-weave intergrowth with chalcopyrite lamellae, generally interpreted as an exsolution of chalcopyrite resulting from an excess of sulfur and iron in the host bornite. Such compositionally anomalous bornite could be a metastable “redbed copper” bornite formed initially during rapid crystallization at low temperatures. During subsequent mild annealing, as could occur during burial to modest depths, oriented chalcopyrite lamellae may have formed along the crystallographic planes of bornite. Brown (1971) showed that annealing at a temperature of 75°C over 24 h was

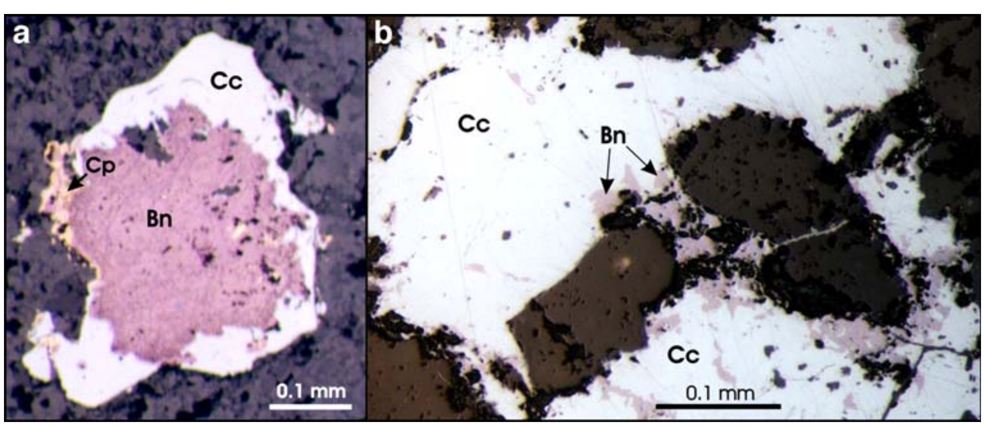

Fig. 16 **a** Purple bornite (*Bn*) partially replaced by chalcocite (*Cc*). **b** Large anhedral chalcocite grains, enclosing remnants of purple bornite. Reflected, plane-polarized light

sufficient to incite an exsolution of chalcopyrite from the pink bornite of the White Pine deposit. The existence of a natural chalcopyrite exsolution at Juramento suggests then that the mineralization formed at low (redbed) temperatures and was subsequently heated naturally (during deep burial and/or tectonic deformation) to produce the exsolution texture.

The most common sulfides associated with bornite are chalcocite and digenite. Where chalcocite or digenite rims bornite, the bornite is typically the purple (i.e., copper-rich) variety (Fig. 16a). Bornite (especially the pink variety) also forms boundary contacts with paragenetically earlier sulfides such as sphalerite, galena, and chalcopyrite (see above). Inclusions of remnant pyrite are rare but not uncommon.

Chalcocite is a common disseminated copper-rich sulfide filling primary intergranular porosities in the lower Yacoraite Formation, where it is generally subordinate in abundance to bornite; it may be the dominant or sole cupriferous sulfide in the upper Lecho Formation. Examined in detail, some apparent chalcocite is, in fact, bluish in reflected light and should be identified as digenite, especially where associated with bornite. In greater detail, especially where seen under high-power oil immersion, the so-called chalcocite can be seen to consist of intimate intergrowths composed of chalcocite, digenite, and possibly djurleite. Aside from cases where digenite is seen clearly to rim or replace bornite, most digenite has been described and discussed in this paper under the term "chalcocite."

Typically, individual chalcocite grains are irregular in shape and of variable size, ranging from 10 to more than 200 μm in size (Fig. 16b). It is observed as rims around all paragenetically earlier sulfides (pyrite, sphalerite, galena, tetrahedrite, chalcopyrite, and bornite) and is not seen as inclusions in those sulfides. The sulfides most commonly associated with chalcocite are bornite (generally the purple type) (Fig. 16) and, less commonly, chalcopyrite.

Primary sulfide zoning

As seen in drill core penetrating well below the effects of surficial oxidation (Fig. 17a), the spatial distributions of pre-ore pyrite and ore-stage sphalerite, galena, and cupriferous sulfides outline a general trend from more chalcophile minerals (or sulfophile metals) in the basal portions of the Yacoraite Formation to less chalcophile minerals at higher stratigraphic levels: from a copper sulfide (or Cu)-dominant zone in basal strata of the Yacoraite to an overlying galena (or Pb)-dominant zone, to a sphalerite (or Zn)-dominant, and finally a pyrite (Fe)-dominant zone. A lateral zoning of sulfide is also apparent in one drill core that happens to lie subparallel to bedding over a distance of about 100 m in the

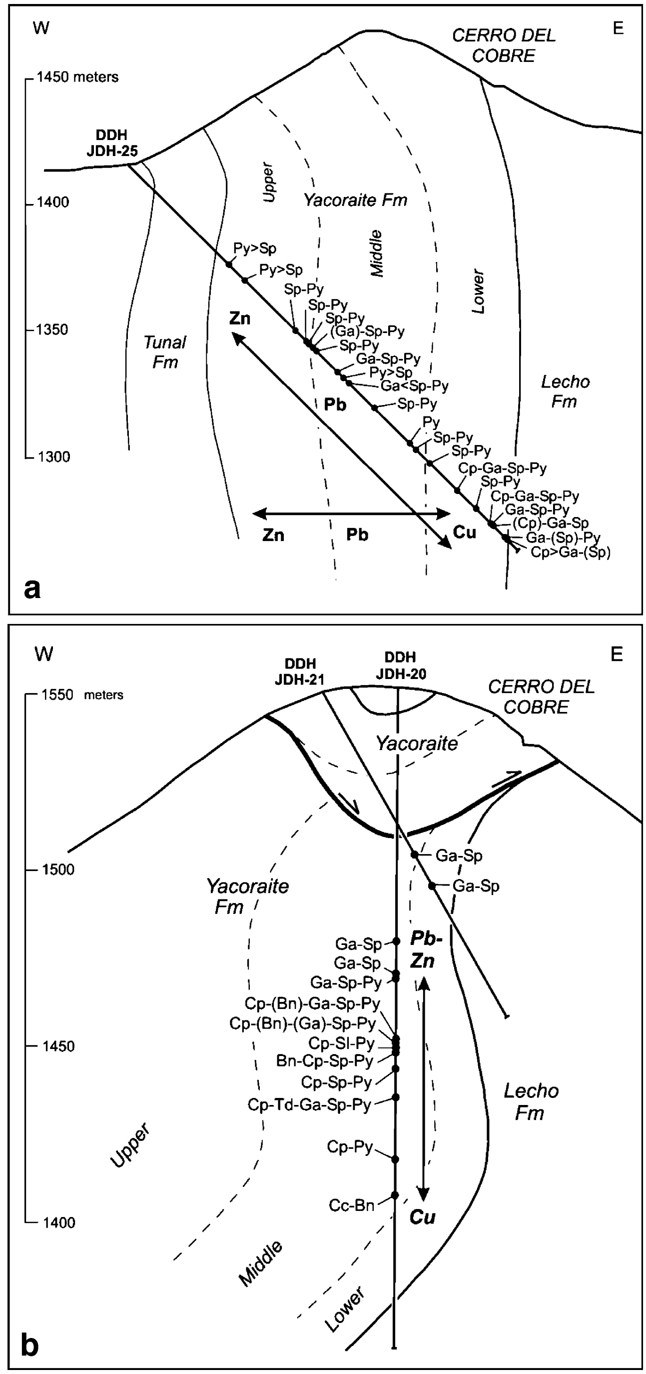

Fig. 17 Cross-sections of zoned primary mineralization in the Yacoraite Formation on Cerro del Cobre, as determined from surface mapping and diamond-drill hole logs. The near-surface rock has experienced supergene alteration to depths averaging about 50–70 m. At greater depths, the dominant primary sulfide mineralogy of drill cores is identified. **a** Copper-rich primary sulfide assemblages in the lower Yacoraite Formation, with progressively more lead- and zinc-rich assemblages stratigraphically upward. **b** Zoning of primary sulfides in a drill core paralleling the lower-middle Yacoraite strata, suggesting a progressive, stratigraphically *lateral*, sulfide zoning from copper-rich to galena-dominant assemblages along the bedding

lower middle Yacoraite Formation (Fig. 17b). All stratigraphically upward, oblique, and lateral transitions are gradual and characterized by broad overlaps of adjacent sulfide zones. The overall zoning of primary sulfides (and metals) is depicted in Fig. 18.

A similar broad zoning is evident among the principal cupriferous sulfides. Chalcocite is generally positioned beneath bornite that is, in turn, located beneath chalcopyrite. Tetrahedrite is most commonly found with chalcopyrite and galena at the upper limit of the cupriferous zone.

Post-ore features

The emplacement of ore-stage minerals in the lower to middle Yacoraite strata apparently terminated with a silicification event that effectively eliminated the porosity and permeability of the shallow-water carbonate–siltstone host rocks. Subsequent post-ore events are related to advanced burial diagenesis, tectonic overprinting (including late fracturing of the host rocks and infiltration of hydrocarbons), and continuing supergene alteration (Fig. 9).

Post-ore silicification consists mainly of quartz and, to a lesser extent, K-feldspar that replaced the outer layers of ooids and partially preserved these structures from subsequent deformation during deep burial compaction. At the same time, authigenic quartz (characterized in some cases by remnant inclusions of carbonates) filled intergranular pores (Fig. 6), replaced portions of oolites, and formed overgrowths on them.

Hydrocarbons are observed in the intergranular porosity of the more permeable rock types (e.g., grainstone and packstone), especially in the coarser-grained fractions of the host rock. Still more commonly, hydrocarbons are associated with fractures cross-cutting all lithologies and along structures including allochems, cements, and matrix material (Fig. 19). The hydrocarbons remain soft and tarry. They are interpreted to post-date the formation of fractures generated during late tectonic deformation; no evidence is found to suggest that base-metal deposition overlapped with this later tectonic deformation or with the generation and migration of hydrocarbons in the Yacoraite Formation.

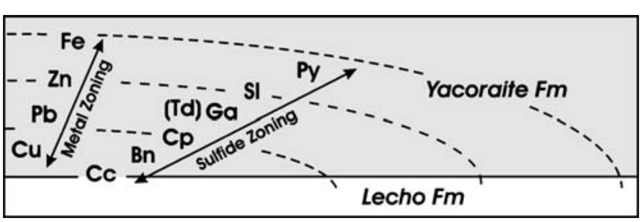

Fig. 18 Schematic illustration of the stratigraphically vertical, oblique, and lateral zoning of base metals and their principal sulfides across the uppermost Lecho Formation and the Yacoraite Formation

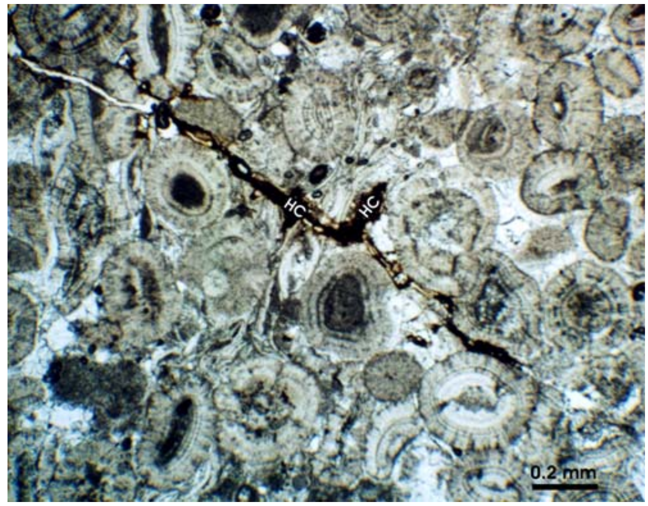

Fig. 19 Hydrocarbons (*HC*) in fracture. Transmitted, plane-polarized light (identify the staining in *upper right*)

Post-ore Andean tectonic deformation has been important at Juramento. As evident in Fig. 17, the Yacoraite and Lecho strata and their sediment-hosted mineralization are folded, tilted, and faulted, and consequently, the usually attractive lateral continuity of SSC-type mineralization has been disrupted severely. Andean tectonism has also been responsible for the location of the Juramento mineralization in elevated, deeply eroded foothill terrain. As a result, exploration at Juramento has focused mainly on the definition of segmented SSC deposits that could be mined from local open pits.

Supergene alteration is generally modest in vertical extent at Juramento, probably due in large part to rapid rates of erosion; boulders with primary chalcocite cementing Lecho sandstone are exposed on steep slopes at high elevations. Oxidation is most obvious and pervasive as malachite staining on mineralized outcrops and as goethite staining where overlying Yacoraite strata were originally pyritic. Seen from a distance, the mineralized Yacoraite strata are typically greenish, in contrast to underlying Pirgua redbeds and overlying buff-colored unmineralized Yacoraite beds. In drill core, oxidation decreases in intensity down to depths of about 70 m. Oxidation is most prominent and typically accompanied by a gypsum cement in strata having high porosities.

Supergene mineralization consists mainly of copper carbonates (especially malachite and azurite), lead and zinc carbonates and sulfates (e.g., cerussite, smithsonite and anglesite), and iron and manganese oxides (e.g., limonite, hematite, and pyrolusite). Malachite prominently replaces copper sulfides, as evident in the upper parts of Cerro del Cobre and Cerro del Plomo where extensive outcrops of well-mineralized lower Yacoraite and upper Lecho formations are stained with a characteristic greenish color. Both malachite and, to a lesser extent, azurite form rims over chalcocite, bornite, and chalcopyrite exposed on outcrops, and fill dissolution cavities in grainstones. The presence of azurite with malachite is consistent with a hot arid climate.

Secondary copper sulfides are most evident in polished sections in the form of digenite and covellite rimming and penetrating primary chalcocite, bornite, and chalcopyrite. Supergene digenite is observed in samples only from the deepest levels of oxidation, where it occurs as rims on primary bornite and chalcopyrite and as overgrowths on sphalerite and galena. In thin sections, goethite is a by-product of the supergene replacement of ferruginous copper sulfides such as bornite and chalcopyrite.

Manganese oxides (e.g., pyrolusite) occur on bedding planes, especially forming black dendritic patterns on outcrops. Iron oxides and hydroxides fill voids left by former cubes of primary pyrite and give a buff color to otherwise grayish unmineralized Yacoraite carbonate rocks.

Sulfur isotope analyses

Concentrates of disseminated pyrite and of base-metal mineralization were prepared for sulfur isotope analyses to compare isotopic ratios with the generally broad range of negative values found in other well-known SSC deposits. Sulfide separation was done by dissolution of sulfide-bearing carbonate-dominant host rock with 10% hydrochloric acid, followed by filtration of the residue onto micropore filters and hand picking of dark opaque grains. The possibility of contamination by sulfates (e.g., gypsum) is not excluded in these preliminary analyses. The samples were labeled according to the dominant sulfide identified in corresponding polished sections. Pyrite-rich samples were subdivided into coarse- and fine-grained material. Analyses were carried out at the G.G. Hatch Laboratory, University of Ottawa, Canada.

The results (Fig. 20; Table 1) identify clearly the pyritic samples as isotopically light (ranging from −45 to −25‰ $\delta^{34}S_{CDT}$; n=6) and characteristic of the light and broad range of sulfur isotopic ratios noted in many SSC deposits (e.g., White Pine; Burnie et al. 1972) and of pyrite formed during early diagenesis as a result of biogenic fractionation (Ohmoto and Rye 1979). No clear distinction exists between coarse- and fine-grained pyrite. The mineralized samples (sphalerite, chalcopyrite, and bornite dominant, as well as one sample containing approximately equal quantities of chalcopyrite, galena, and sphalerite) are distinctly heavier than pyrite (ranging from −25 to −5‰ $\delta^{34}S_{CDT}$). There are no obvious distinctions between the isotopic compositions of the various ore-stage minerals.

Because the base-metal sulfides generally show replacement of pyrite to be a prominent means of copper–lead–zinc emplacement, the ore sulfides could be expected to have sulfur isotopic compositions resembling those of the replaced pyrite. The heavier isotopic compositions of the base-metal mineralized samples relative to pyrite despite textural evidence of pyrite replacement may indicate that a fraction of the sulfur for ore sulfide deposition was extracted from a sulfate such as gypsum; the position of the base-metal sulfide ratios between the light isotopic compositions of pyrite and the presumably heavier compositions of a common sulfate such as gypsum suggests a mixing process. The replacement of blade-like gypsum by ore-stage sulfides has been confirmed (Fig. 15), but that process does not require that the sulfate sulfur from gypsum was incorporated into the replacing sulfides. In fact, the low-temperature reduction of sulfate to sulfide would presumably require an anoxic bacterial activity during the emplacement of base metals, subsequent to the earlier formation of syndiagenetic pyrite; the contemporaneous

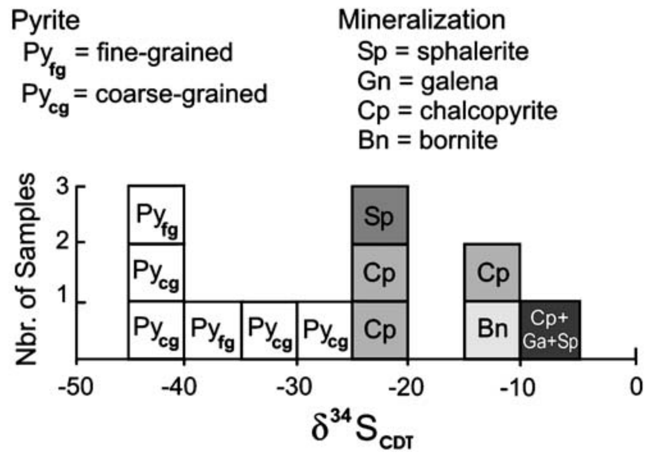

Fig. 20 Sulfur isotope analyses for pyrite and ore-stage base-metal sulfides. See text for discussion

Table 1 Sulfur isotopic compositions of pyrite and ore-stage sulfides

Number	Composition	$\delta^{34}S_{CDT}$
Pyrite		
1	Coarse grained	−27.7
2	Fine grained	−39.3
3	Fine grained	−42.1
4	Coarse grained	−31.9
5	Coarse grained	−42.6
6	Coarse grained	−42.9
Ore-Stage Sulfides		
7	Chalcopyrite	−12.0
8	Bornite	−10.4
9	Chalcopyrite	−21.9
10	Chalcopyrite	−24.9
11	Chalcopyrite–galena–sphalerite	−8.0
12	Sphalerite	−24.8

presence of bacterial activity and noxious metals seem unlikely.

The heavy sulfur isotopic ratios for ore-stage sulfides relative to the average ratio for replaced pyrite might also be attributed to isotopically heavy sulfate introduced in the ore-forming fluid, as proposed by Hoy and Ohmoto (1989). However, the reduction of that sulfate to sulfide would be difficult, given that contemporaneous bacterial activity has been ruled out (above) and that thermochemical reduction is very slow at low temperatures (Ohmoto and Goldhaber 1993).

The lack of a narrow range of isotopic compositions for ore-stage sulfides indicates that the chief source of sulfur was not a homogeneous fluid such as a natural sour gas containing reduced sulfur (H_2S). A sour gas source would have the advantage of providing already reduced sulfur, but the production of a natural gas from the Yacoraite (Mon and Salfity 1995) would presumably require prior burial to a level deeper than that necessary to generate natural gas and well beyond that necessary for post-ore stylolitization. Alternatively, the samples submitted for analysis may have remained contaminated to various degrees by gypsum not totally removed during sample preparation.

Discussion

Detailed studies of SSC deposits have repeatedly led to the conclusion that the ore-stage metals were introduced after sedimentation, and in many cases, this mineralization is found to have pre-dated significant deformation, other than early deformations that may have accompanied synsedimentary faulting in the host rift basins (see, for example, Bartholomé (1962, 1974) for the well-preserved Kolwezi portion of the Central African Copperbelt; Brown (1971) for the main-stage sulfide facies mineralization at White Pine, Michigan; Chartrand and Brown (1985) for the Redstone deposit of the Northwest Territories, Canada; and Rentzsch (1974) and Jowett (1986) for major portions of the Kupferschiefer mineralization). The genesis of such mineralization is commonly said to have taken place during diagenesis of the host sediments.

More complex interpretations are commonly proposed where the host rocks have experienced the overprint of orogenic deformation and metamorphism and where the sediment-hosted mineralization typically includes both disseminated sulfides and vein sulfides (see, for example, Selley et al. (2005) for the Zambian portion of the Central African Copperbelt). Sulfide minerals and their textures may be interpreted to be primary and contemporaneous with orogenesis, and their emplacements are commonly said to be related to deep structural pathways for ore fluid flow (e.g., Bechtel et al. 2001; Blundell et al. 2003; Muchez et al. 2005; McGowan et al. 2006). Unfortunately, most, if not all, minerals and textures are ambiguous or conflicting (Selley et al. 2005, p. 982) and may have resulted from synorogenic recrystallization and/or local remobilization of earlier so-called diagenetic sulfides, as recognized by Hitzman et al. (2005). Fortunately, at Juramento, most deep primary sulfide mineralization has not been significantly modified by Andean orogenesis at the hand specimen and microscopic scales. Host sedimentary units are tilted, isoclinally folded, and faulted (Figs. 4 and 17), but metamorphic effects have been negligible, and original low-temperature minerals and textures are well preserved.

Prior to this study, the classification of the Juramento copper–silver deposit as SSC-type mineralization was based largely on general rather than definitive aspects. For example, the mineralization was known to be composed mainly of disseminated fine-grained cupriferous sulfides widespread along basal sandstones, mudstones, and oolitic and stromatolitic carbonates immediately overlying a thick sequence of continental rift-filling redbeds. Sufficient parallels could be seen with major SSC districts such as the Kupferschiefer and the Central African Copperbelt to justify the exploration programs of Pecomrio in the 1970s and Paramount in the 1990s. At the same time, however, numerous reviews and compilations of worldwide occurrences of SSC mineralization tended to give minimal recognition to the copper deposits of the Salta rift basins or they omitted their mention altogether (e.g., Gustafson and Williams 1981; Boyle et al. 1989). The global compilation of Kirkham et al. (1994) was among the earliest of publications to identify the Juramento deposit as SSC-type mineralization.

The more detailed descriptions and interpretations of the Juramento deposit presented in this paper show clearly that the Juramento mineralization qualifies as a full member of the SSC deposit type; generally accepted diagenetic characteristics of the SSC deposit type may be found in Boyle et al. (1989), as well as in the overviews and compilations of Jowett (1991), Brown (1992, 1997a), Kirkham et al. (1994), Kirkham (1995), Cox et al. (2003), and Hitzman et al. (2005). Briefly stated, the Juramento mineralization exhibits the following attributes at the deposit scale: (1) The host rocks are graybeds (mainly shallow-water carbonate siltstones and mudstones and a basal sandstone, including abundant stromatolites); (2) the footwall consists of immature, coarse-grained, rift-filling redbeds as well as some basaltic units, forming a well-defined redox boundary next to the overlying graybeds; (3) the mineralization consists of disseminated fine-grained cupriferous sulfides, accompanied by other base-metal sulfides (mainly galena and sphalerite) common to SSCs; (4) the sulfides are zoned, with the more sulfophile cupriferous minerals proximal to the redox boundary and least sulfophile sulfides (galena, sphalerite, and pyrite) in distal positions; (5) ore-stage sulfides replace earlier fine-grained syndiagenetic pyrite; (6) the overall array of sulfide minerals exhibits a progressive paragenetic sequence of emplacement from pre-ore pyrite to ore-stage sulfides (sphalerite, galena, and then cupriferous sulfides), and the paragenetic sequence among the cupriferous sulfides passes from chalcopyrite to bornite to chalcocite; and (7) the overall configuration of the mineralized zone appears to be moderately cross-cutting relative to the host-rock bedding.

In general, the configuration of the mineralized zone and its position immediately adjacent to a stratigraphically defined redox boundary, together with the sulfide zoning and replacement textures, indicate an overprint of copper (and accompanying metals: lead, zinc, silver, arsenic, antimony) on originally pyritic graybeds. This concept suggests that the ore-stage metals entered the basal Lecho and Yacoraite strata from the underlying Pirgua redbeds, consistent with the general genetic model for SSC mineralization (Brown 1992, 1997a; Kirkham 1989, 1995). Evidence for reducing conditions and early pyrite formation within the graybeds (e.g., stromatolites in the Yacoraite carbonates that would have been rich in immature organic matter and, thus, conducive to anaerobic bacterial activity and the biogenic production of sulfide) suggests, as well, that the introduced metals would have been readily precipitated as sulfides upon encountering pre-ore pyrite in the basal graybeds. Preliminary sulfur isotopic analyses suggest that the sulfur of ore-stage minerals is moderately heavier than that of replaced pyrite, but it is difficult to attribute the heavy sulfur (a) to gypsum or sulfates in the ore-fluid because the means to reduce sulfate sulfur at low temperatures are not evident, or (b) to a sour gas because burial to the gas window should not have occurred until well after early diagenetic base-metal mineralization. The accumulation of several ore-stage sulfides (e.g., sphalerite, bornite, and chalcopyrite) along stylolites indicates that mineralization pre-dated advanced stages of host-rock compaction and diagenesis (Fig. 9). More precisely, the documented silicification of the host strata before that compaction (Fig. 9) may well have terminated the introduction of base metals into the basal Juramento Formation; this silica would have closed pores and could have effectively prevented the further influx of ore-forming metalliferous brines.

The regional geological setting of the Juramento deposit is also consistent with its assignment to the SSC deposit type. First, SSCs are recognized as a post-oxyatmoversion (i.e., post-2.4 Ga approximately; Roscoe 1973, Kirkham and Roscoe 1993) deposit type (Meyer 1981), ostensively due to the need for an oxygenated atmosphere to produce oxygenated subsurface brines capable of transporting copper in low-temperature aqueous solutions (Brown 1971, 2003, 2005; Rose 1976, 1989; Kirkham 1989). The Late Cretaceous age of the Juramento host rocks assures that the Juramento mineralization qualifies on this basis.

Second, the Juramento mineralization is hosted by a major continental rift system, as are all significant SSCs (Brown 1984, 1992, 1997a, b; Jowett 1989; Jowett et al. 1987; Kirkham 1989, 1995; Hitzman et al. 2005). This feature assures that large amounts of copper may have been leached by an oxygenated brine from the trace amounts available throughout the footwall Pirgua redbeds. Although probably not essential to the formation of SSC mineralization, the presence of bimodal basalts within the Salta rift basins may also have been a favorable feature, perhaps adding to the copper that could have been leached from mafic minerals in the footwall units, or perhaps signaling anomalous amounts of magmatic heat in an otherwise cold rift-basin fill.

Finally, Kirkham (1989) has shown that SSCs are closely associated on a global basis with evaporitic sediments formed in hot arid climates at low paleolatitudes; evaporites could be responsible for the high salinity of the footwall pore fluid. Again, the Juramento deposit qualifies because the Yacoraite carbonates contain gypsum blades typical of shallow-water carbonates formed under hot arid conditions (Kinsman 1969; Kendall 1992), while the region was located at a latitude of about 30°S in Late Cretaceous time (Kirkham 1989, his Fig. 11). Furthermore, evaporitic units are extensive in the upper lacustrine strata of the Salta rift basins (Gómez et al. 1989).

Concluding remarks

Once established as hosting SSC-type mineralization, the Juramento property (and other portions of the Salta rift basin system) might be expected to host major or even world-class orebodies. After all, the Central African Copperbelt and the Kupferschiefer contain numerous world-class ore deposits and even second-level SSC deposits, such as White Pine, Michigan, have also been very important mineral deposits. The fundamental economic attraction of this deposit type lies first in the typically widespread mineralization along bedding and hopefully over several meters of stratigraphic thickness, resulting in large tonnage mineral deposits. At the same time, the metal grades may be considerably higher than those commonly found in other world-class copper deposits (e.g., commonly well above those of porphyry copper deposits; Kirkham 1989, 1994, 1995; Singer 1995). In the case of the Juramento deposit, the mineralized zone commonly measures several meters in thickness, but the overall grades are 1% Cu or less, with only short core intervals attaining or exceeding 2% Cu. Silver (approximately 20 g/t) could add about 15% copper equivalent to the value of the deposit.

Combining the recognition of the Juramento deposit as SSC-type mineralization with the normal economic attractions of mineralization of this type (especially high tonnages and good copper grades), it is reasonable to expect that economic deposits will yet be defined within the very extensive Salta rift system. Two aspects of the Juramento deposit may be cited to encourage further exploration. First, the exposure of mineralization at Juramento (Fig. 4) is small compared to the vast lateral extent of the favorable host strata (Fig. 1). Second, the favorable shallow-water facies exposed at Juramento may be marginal to still more favorable deeper water facies in the Salta basins (e.g., carbonaceous Kupferschiefer-type beds). The application of the SSC genetic model to the entire rift system could be very rewarding.

Acknowledgment We are especially appreciative for the invitation from Ian Mason to undertake this study and for his insightful introduction to the field area and for the important support of Joe Rotzien and his most enthusiastic and helpful geos during the fieldwork. We also wish to acknowledge Professors Mountjoy and Williams-Jones of McGill University who provided invaluable advice and access to their research facilities. We also thank Paramount Ventures and Finances for the field employment of the first author and for partial funding of research costs. The study was also sponsored in part by a Natural Sciences and Engineering Research Council of Canada Individual Grant to the second author.

We wish, as well, to thank Alexandre Cabral, Rod Kirkham, and Steven Roberts for the many helpful suggestions provided in their careful reviews of the manuscript, and Bernd Lehmann for his excellent editorial comments.

References

Alexander Mining (2005) Regulatory announcement, Alexander Mining PLC, Operations: Leon copper/silver project, Salta Province, NW Argentina. http://www.londonstockexchange.com/LSECWS/IFSPagesMarketNewsPoppup.aspx?id=1045802&source=RNS

Bartholomé P (1962) Les minerais cupro-cobaltifères de Kamoto (Katanga-Ouest). Pt. I. Pétrographie, Pt. II. Paragenèse. Studia Universitatis "Louvanium", Faculté de Sciences. Leopoldville (Kinshasa) 14:3–40

Bartholomé P (1974) On the diagenetic formation of ores in sedimentary beds, with special reference to Kamoto, Shaba, Zaïre. In: Bartholomé P (ed) Gisements stratiformes et Provinces Cuprifères. Société Géologique de Belgique, Liège, pp 203–213

Bechtel A, Sun Y, Puettmann W, Hoernes S, Hoefs J (2001) Isotopic evidence for multi-stage base metal enrichment in the Kupferschiefer from the Sangerhausen Basin, Germany. Chem Geol 176:31–49

Blundell DJ, Karnkowski PH, Alderton DHM, Oszczepalski S, Kucha H (2003) Copper mineralization of the Polish Kupferschiefer: a proposed basement fault-fracture system of fluid flow. Econ Geol 98:1487–1495

Boyle RW, Brown AC, Jefferson CW, Jowett EC, Kirkham RV (eds) (1989) Sediment-hosted stratiform copper deposits. Geological Association of Canada, Special Paper 36:710

Brett R, Yund RA (1964) Sulfur-rich bornites. Am Mineral 49:1084–1098

Brown AC (1971) Zoning in the White Pine copper deposit, Ontonogan County, Michigan. Econ Geol 66:543–573

Brown AC (1984) Alternative sources of metals for stratiform copper deposits. Precambrian Res 25:61–74

Brown AC (1992) Sediment-hosted stratiform copper deposits. Geosci Can 19:125–141 [reprinted in Sheahan P, Cherry ME (eds) (1993) Ore deposit models. Geol Assoc Can 2(Reprint Series 6): 99–115]

Brown AC (1997a) World-class sediment-hosted stratiform copper deposits: characteristics, genetic concepts and metallotects. Aust J Earth Sci 44:317–328

Brown AC (1997b) Global-scale constraints on the formation of sediment-hosted stratiform copper deposits. In: Charlet JM (ed) Stratabound copper deposits and associated mineralization. Proceedings, International Cornet symposium, Mons, pp 93–102

Brown AC (2003) Redbeds: source of metals for sediment-hosted stratiform copper, sandstone copper, sandstone lead, and sandstone uranium–vanadium deposits. In: Lentz DR (ed) Geochemistry of sediments and sedimentary rocks: evolutionary considerations to mineral deposit-forming environments. Geol Assoc Can Geotext 4:121–133

Brown AC (2005) Refinements for footwall red-bed diagenesis in the sediment-hosted stratiform copper deposits model. Econ Geol 100:765–771

Burnie SW, Schwartz HP, Crockett JH (1972) A sulfur isotopic study of the White Pine mine, Michigan. Econ Geol 67:895–914

Chartrand FM, Brown AC (1985) The diagenetic origin of stratiform copper mineralization, Coates Lake, Redstone Belt, NWT, Canada. Econ Geol 80:325–343

Cox DP, Lindsey DA, Singer DA, Diggles MF (2003) Sediment-hosted copper deposits of the world: deposit models and database. US Geological Survey, Open-file report 03-107, 50 p

Durieux CG (2000) Diagenetic mineralization of the Juramento sediment-hosted stratiform Cu–(Ag) deposit, Salta district, northeastern Argentina. M.Sc.A. thesis, École Polytechnique de Montréal, Montreal, 152 p

Espisúa E, Amengual R (1983) Juramento, un deposito estratoligado de cobre, plata y plomo, Provincia de Salta, República Argentina. Segundo Congreso Nacional de Geología Económica, San Juan. Actas 1:71–90

Friedman GM, Sanders JE (1978) Principles of sedimentology. Wiley, New York

Friedman GM, Amiel AJ, Braun M, Miller DS (1973) Generation of carbonate particles and laminites in algal mats; example from sea-marginal hypersaline pool, Gulf of Aqaba, Red Sea. AAPG Bull 57:541–557

Friedman GM, Sanders JE, Kopaska-M DC (1992) Principles of sedimentary deposits. Macmillan, New York

Gómez Omil RJ, Boll A, Hernández RM (1989) Cuenca cretácico–terciária del noroeste Argentino (grupo Salta). In: Chebli G, Spalletti L (eds) Cuencas sedimentarias Argentinas, Universidad Nacional de Tucuman, Tucuman, Argentina. Ser Correl Geol 6:43–64

Greensmith JT (1989) Petrology of the sedimentary rocks, 7th edn. Unwin Hyman, London

Gustafson LB, Williams N (1981) Sediment-hosted stratiform deposits of copper, lead and zinc. In: Skinner BJ (ed) 75th Anniversary volume. Economic Geology Publication, El Paso, pp 139–178

Hitzman M, Kirkham R, Broughton D, Thorson J., Selly D (2005) The sediment-hosted stratiform copper ore system. In: Thompson JFH, Goldfarb RJ, Richards JP (eds) 100th Anniversary volume. Society of Economic Geologists, pp 609–642

Hoy LD, Ohmoto H (1989) Constraints for the genesis of redbed-associated stratiform Cu deposits from sulphur and carbon mass-

balance relations. In: Boyle RW, Brown AC, Jefferson CW, Jowett EC, Kirkham RV (eds) Sediment-hosted stratiform copper deposits. Geological Association of Canada, Special Paper 36:135–149
James NP (1984) Shallowing-upward sequences in carbonates. In: Walker RG (ed) Facies models. Geological Association of Canada, Geoscience Canada Reprint Series 1:213–228
Jordan TE, Alonso RN (1987) Cenozoic stratigraphy and basin tectonics of the Andes Mountains, 20°–29° south latitude. AAPG Bull 71:49–64
Jowett EC (1986) Genesis of Kupferschiefer Cu–Ag deposits by convective flow of Rotliegende brines during Triassic rifting. Econ Geol 81:1823–1837
Jowett EC (1989) Effects of continental rifting on location and genesis of stratiform copper–silver deposits. In: Boyle RW, Brown AC, Jefferson CW, Jowett EC, Kirkham RV (eds) Sediment-hosted stratiform copper deposits. Geological Association of Canada Special Paper 36:53–66
Jowett EC (1991) The evolution of ideas about the genesis of stratiform copper–silver deposits. Monogr Econ Geol Pub 8:117–132
Jowett EC, Rydzewski A, Jowett RJ (1987) The Kuperferschiefer Cu–Ag ore deposits in Poland: a reappraisal of the evidence of their origin and presentation of a new genetic model. Can J Earth Sci 24:2016–2037
Kendall RL (1969) The ecological history of the Lake Victoria basin. Ecol Monogr 39:121–176
Kendall AC (1992) Evaporites. In: Walker RG, James NP (eds) Facies models: response to sea level change. Geological Association of Canada, pp 375–409
Kinsman DJJ (1969) Modes of formation, sedimentary associations, and diagnostic features of shallow-water and supratidal evaporite. Am Assoc Pet Geol Bull 53:830–840
Kirkham RV (1989) Distribution, setting and genesis of sediment-hosted stratiform copper deposits. In: Boyle RW, Brown AC, Jefferson CW, Jowett EC, Kirkham RV (eds) Sediment-hosted stratiform copper deposits. Geol Assoc Can Special Paper 36:3–38
Kirkham RV (1995) Sediment-hosted stratiform copper. In: Eckstrand OR, Sinclair WD, Thorpe RI (eds) Geology of Canadian mineral deposit types. Geol Surv Can Geol Canada 8:223–240 (also Geological Society of America, the Geology of North America, vol. P-1)
Kirkham RV (1996) Exploration for stratabound copper deposits in the Salta area, northwestern Argentina. Unpublished private report for Paramount Ventures and Finance, p 16
Kirkham RV, Roscoe SM (1993) Atmospheric evolution and ore deposit formation. Resour Geol Special Issue 15:1–17
Kirkham RV, Carrière JJ, Laramée RM, Garson DF (1994) Global distribution of sediment-hosted stratiform copper deposits and occurrences. Geol Surv Can, open file 2915b, 256 p (with map and accompanying notes)
Marquillas RA (1984) La Formación Yacoraite (Crétacico Superior) en el Río Juramento, Salta: Estratigrafía y Ciclicidad. Noveno Congreso Geológico Argentino, S. C. de Bariloche. Actas 5:186–196
Marquillas RA, Salfity JA (1988) Tectonic framework and correlations of the Cretaceous–Eocene Salta Group; Argentina. In: Bahlburg H, Breitkreutz C, Giese L (eds) The Southern Central Andes. Lect Notes Earth Sci 17:119–136
Marquillas RA, Boso MA, Salfity JA (1984) La formación Yacoraite (Cretácico Superior) en el Norte Argentino, al Sur del paralelo 24°. Noveno Congreso Geológico Argentino, S. C. de Bariloche. Actas 2:300–310
Mason IM (1996) Juramento property, Argentina, report of 1995 exploration. Paramount Ventures and Finance, unpublished interim report, 48 p
McGowan RR, Roberts S, Boyce AJ (2006) Origin of the Nchanga copper–cobalt deposits of the Zambian copperbelt. Miner Depos 40:617–638
Meyer C (1981) Ore-forming processes in geologic history. In: Skinner BJ (ed) 75th Anniversary volume. Economic Geology Pub, El Paso, pp 6–41
Mon R, Salfity JA (1995) Tectonic evolution of the Andes of northern Argentina. In: Tankard AJ, Suarez R, Welsink HJ (eds) Petroleum basins of South America. Mem Am Assoc Pet Geol 62:269–283
Muchez P, Heijlen W, Banks D, Blundell D, Boni M, Grandia F (2005) Extensional tectonics and the timing and formation of basin-hosted deposits in Europe: geodynamics and ore deposit evolution in Europe. Ore Geol Rev 27:241–267
Ohmoto H, Goldhaber MB (1993) Sulfur and carbon isotopes. In: Barnes HL (ed) Geochemistry of hydrothermal ore deposits, 3rd edn. Wiley, New York, pp 517–611
Ohmoto H, Rye RO (1979) Isotopes of sulfur and carbon. In: Barnes HL (ed) Geochemistry of hydrothermal ore deposits, 2nd edn. Wiley, New York, pp 509–567
Palma RM (1984) Interpretación ambiental de las formaciones del límite Cretácico–Terciario en el perfil Esquina Blanca, (Dpto. Humahuaca, Provincia de Jujuy). Noveno Congreso Geológico Argentino, S. C. de Bariloche. Actas 1:420–436
Platt NH, Wright VP (1991) Lacustrine carbonates: facies models, facies distribution and hydrocarbon aspects. In: Anadon P, Cabrera L, Kelts K (eds) Lacustrine facies analysis. Int Assoc Sedimentol Special Publication 13:57–74
Ramdohr P (1969) The ore minerals and their intergrowth. Pergamon, Braunschweig
Reading HG (1982) Sedimentary basins and global tectonics. Proc Geol Assoc 93:321–350
Rentzsch J (1974) The Kupferschiefer in comparison with the deposits of the Zambian copperbelt. In: Bartholomé P (ed) Gisements Stratiformes et Provinces Cuprifères. Société Géologique de Belgique, Liège, pp 395–418
Roscoe SM (1973) The Huronian Supergroup, a Paleoaphebian succession showing evidence of atmospheric evolution. In: Young GM (ed) Huronian stratigraphy and sedimentation. Geol Assoc Can Special Paper 12:32–47
Rose AW (1976) The effect of cuprous chloride complexes in the origin of red-bed copper and related deposits. Econ Geol 71:1036–1048
Rose AW (1989) Mobility of copper and other heavy metals in sedimentary environments. In: Boyle RW, Brown AC, Jefferson CW, Jowett EC, Kirkham RV (eds) Sediment-hosted stratiform copper deposits. Geol Assoc Can Special Paper 36:97–110
Rotzien JL, Wormald PJ (1998) Juramento project: report on 1997 diamond drilling program. Paramount Ventures and Finances, unpublished interim report, 37 p
Ryan RJ, Boehner RC, Stea RR, Rogers PJ (1989) Geology, geochemistry, and exploration applications for the Permo-Carboniferous redbed copper deposits of the Cumberland Basin, Nova Scotia, Canada. In: Boyle RW, Brown AC, Jefferson CW, Jowett EC, Kirkham RV (eds) Sediment-hosted stratiform copper deposits: Geol Assoc Can Special Paper 36:245–256
Salfity JA (1979) Paleogeología de la cuenca del Grupo Salta del norte de Argentina. Sexto Congreso Geológico Argentino. Actas 1:239–255
Salfity JA, Marquillas RA (1994) Tectonic and sedimentary evolution of the Cretaceous–Eocene Salta Group basin, Argentina. In: Salfity JA (ed) Cretaceous tectonics of the Andes. Vieweg, Wiesbaden, pp 266–313
Selley D, Broughton D, Scott R, Hitzman M, Bull S, Large R, McGoldrick P, Croaker M, Pollington N, Barra F (2005) A new look at the geology of the Zambian Copperbelt. In: Thompson

JFH, Goldfarb RJ, Richards JP (eds) 100th Anniversary volume. Society of Economic Geologists, pp 965–1000

Singer (1995) World class base and precious metal deposits—a quantitative analysis. Econ Geol 90:88–104

Sureda RJ, Galisky MA, Arañaraz P, Daroca J (1986) Aspectos metalogénicos del noroeste Argentino, Provincias de Salta y Jujuy. Capricornio 1:39–95

Tucker ME, Wright VP (1990) Carbonate sedimentology. Blackwell, London

Walker TR (1989) Application of diagenetic alterations in redbeds to the origin of copper in stratiform copper deposits. In: Boyle RW, Brown AC, Jefferson CW, Jowett EC, Kirkham RV (eds) Sediment-hosted stratiform copper deposits. Geol Assoc Can Special Paper 36:85–96

Williamson CR, Pickard MD (1974) Petrology of carbonate rocks of the Green River Formation (Eocene). J Sediment Petrol 44: 738–759

Yund RA, Kullerud G (1966) Thermal stability of assemblages in the Cu–Fe–S system. J Petrol 7:454–488

Zielinski A, Bloch S, Walker TR (1983) The mobility and distribution of heavy metals during the formation of first cycle red beds. Econ Geol 78:1574–1589